Critical Thinking in Pumping Test Interpretation

Interpretation of pumping tests in aquifers with linear boundaries

Christopher J. Neville
S.S. Papadopulos & Associates, Inc.
Last update: October 15, 2025

Overview

Although all aquifers are bounded, when we interpret the results of short-term pumping tests, we frequently ignore the presence of boundaries. In many cases of practical significance, neglecting the boundaries may be highly restrictive. It may limit our analysis to the consideration of drawdown from only the first few minutes or hours of pumping. Furthermore, such idealized analyses do not provide much insight into the effects that boundaries may have on the response to pumping.

These notes have been prepared to provide an introduction to the interpretation of pumping tests where boundaries are relatively close to the pumping well. To illustrate some basic concepts, we will consider three idealized cases that are amenable to treatment with an analytical approach:

- Aquifers with one linear constant-head boundary;
- Aquifers with one linear impermeable boundary; and
- Aquifers with two linear impermeable boundaries (channel aquifers).

We recognize from the outset that there may be cases in which complex boundary conditions may not be amenable to such simple analyses. Where boundaries and additional sources/sinks are located relatively close to the pumping well, the analyst may have to develop a numerical model to interpret the drawdown data.

Outline

1. Aquifers with a single linear constant-head boundary

As with all pumping tests, the Theis model is the starting point for the interpretation of tests conducted in bounded aquifers. The Theis problem is linear; neither the coefficients appearing in the governing equation, nor the boundary conditions depend upon the drawdown. The property of linearity has important implications for the interpretation of pumping test data. For linear problems, we can derive solutions to complex problems by adding together solutions for simpler cases, a procedure referred to as *superposition*. Pumping tests conducted near a linear boundary (for example, a stream or a fault) can be interpreted by superposing Theis solutions in space, using what are referred to as *image wells*.

For the case of a linear constant-head boundary, the drawdown along the boundary is zero. As shown in Figure 1, a linear boundary with zero drawdown is simulated with an imaginary well placed an equal distance from the boundary, pumping at a rate equal in magnitude, but opposite in sign, to the actual well.

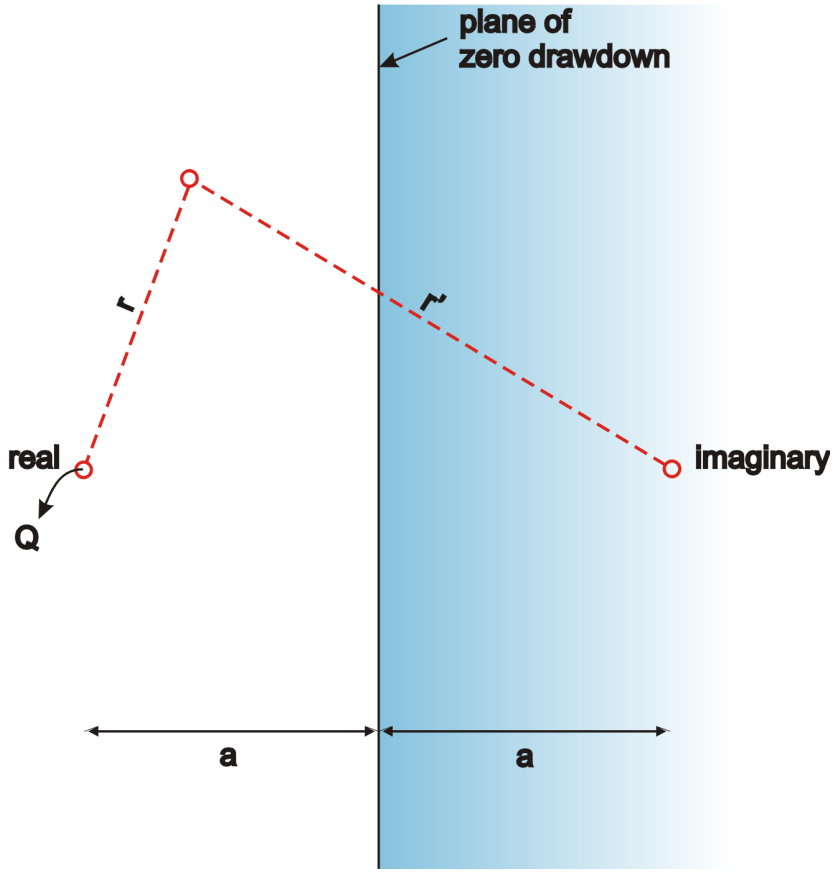

Figure 1. Application of image theory for a single linear constant-head boundary

The drawdown due to the pair of real and imaginary wells is:

$$s = \frac{Q}{4\pi T} W\left(\frac{r^2 S}{4Tt}\right) - \frac{Q}{4\pi T} W\left(\frac{r'^2 S}{4Tt}\right)$$

where r is the distance between the real well and the observation well, and r' is the distance between the imaginary well and the observation well. Example calculations are shown in Figure 2. When a well is pumped near a constant head boundary, we observe two intervals of distinct response. During the early period, the observation well responds as if there were no boundary at all. The drawdown stabilizes after the effects of pumping propagate to the boundary.

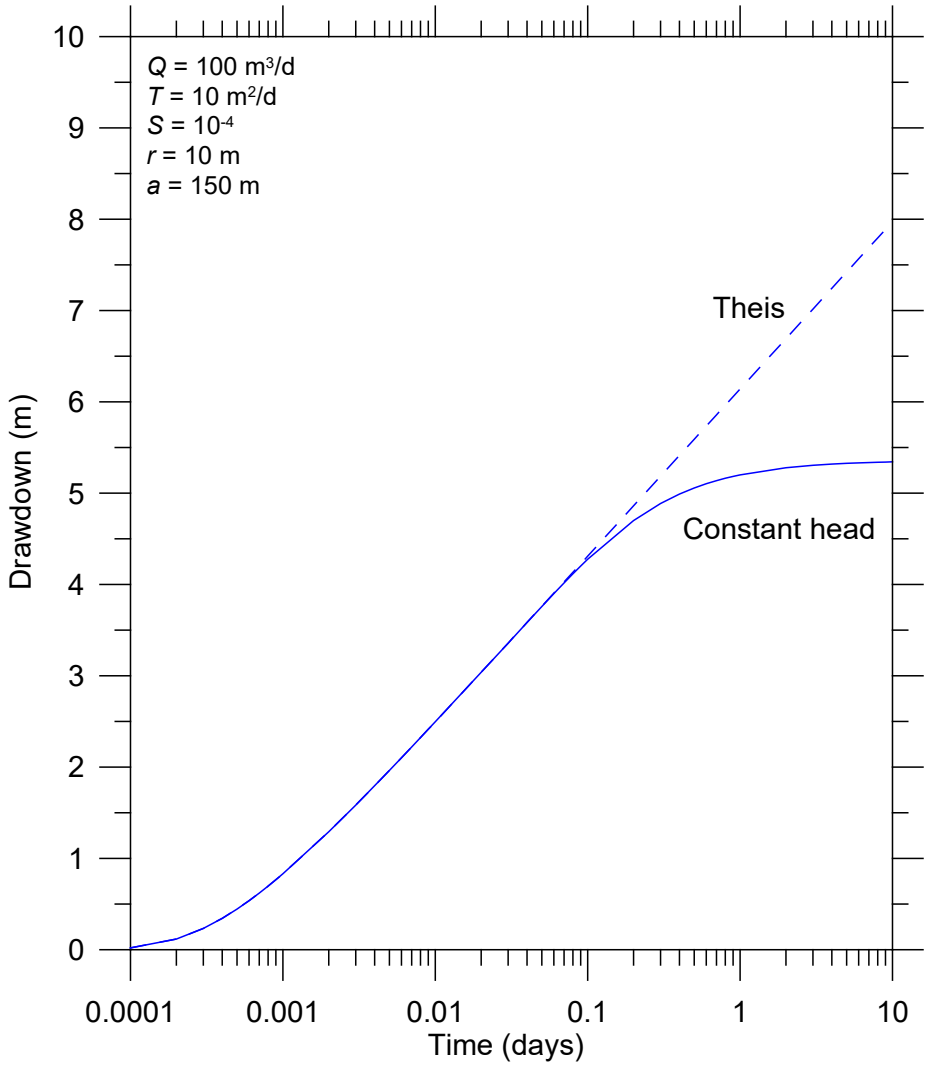

Figure 2. Pumping test in an aquifer with a single linear constant-head boundary

If we use the Cooper-Jacob approximation for the Theis well function, the drawdown is given by:

$$s = \frac{Q}{4\pi T}\left[-0.5772 - ln\left\{\frac{r^2 S}{4Tt}\right\}\right] - \frac{Q}{4\pi T}\left[-0.5772 - ln\left\{\frac{r'^2 S}{4Tt}\right\}\right]$$

Using the properties of the log function, the expanded solution reduces to the simple expression:

$$s = \frac{Q}{4\pi T} ln\left\{\frac{r'^2}{r^2}\right\}$$

$$= \frac{Q}{2\pi T} ln\left\{\frac{r'}{r}\right\} = \frac{Q}{2\pi T} 2.303\, log_{10}\left\{\frac{r'}{r}\right\}$$

The Cooper-Jacob approximation in this case is independent of time.

Late-time derivative

The derivative is defined as:

$$D_t(s) = \frac{\partial s}{\partial(ln\{t\})}$$
$$= \frac{\partial}{\partial(ln\{t\})}\left[\frac{Q}{2\pi T} ln\left\{\frac{r'}{r}\right\}\right] = 0$$

The presence of a constant-head boundary is indicated by a decline in the derivative to a value of zero.

$$D_t(s) \to 0$$

The decline in the derivative is diagnostic of recharge effects acting to attenuate drawdowns. The stabilization of the derivative for a single linear constant-head boundary is shown in Figure 3.

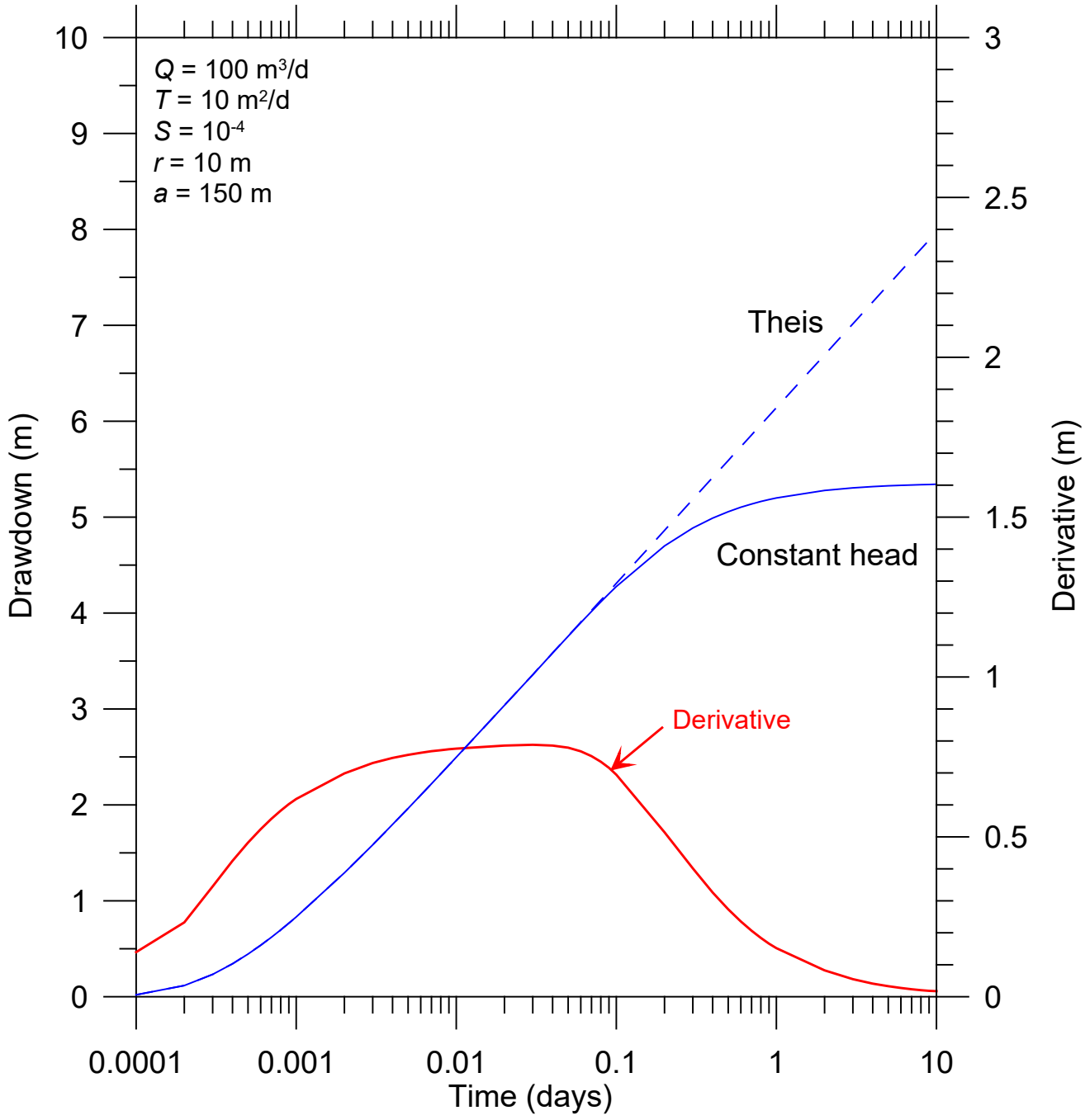

Figure 3. Pumping test in an aquifer with a single linear constant-head boundary

2. Aquifers with a single impermeable boundary

For the case of a linear no-flow boundary, the linear boundary is a line of symmetry. As shown in Figure 4, this is simulated with an imaginary well placed an equal distance from the boundary, pumping at the same rate as the real well.

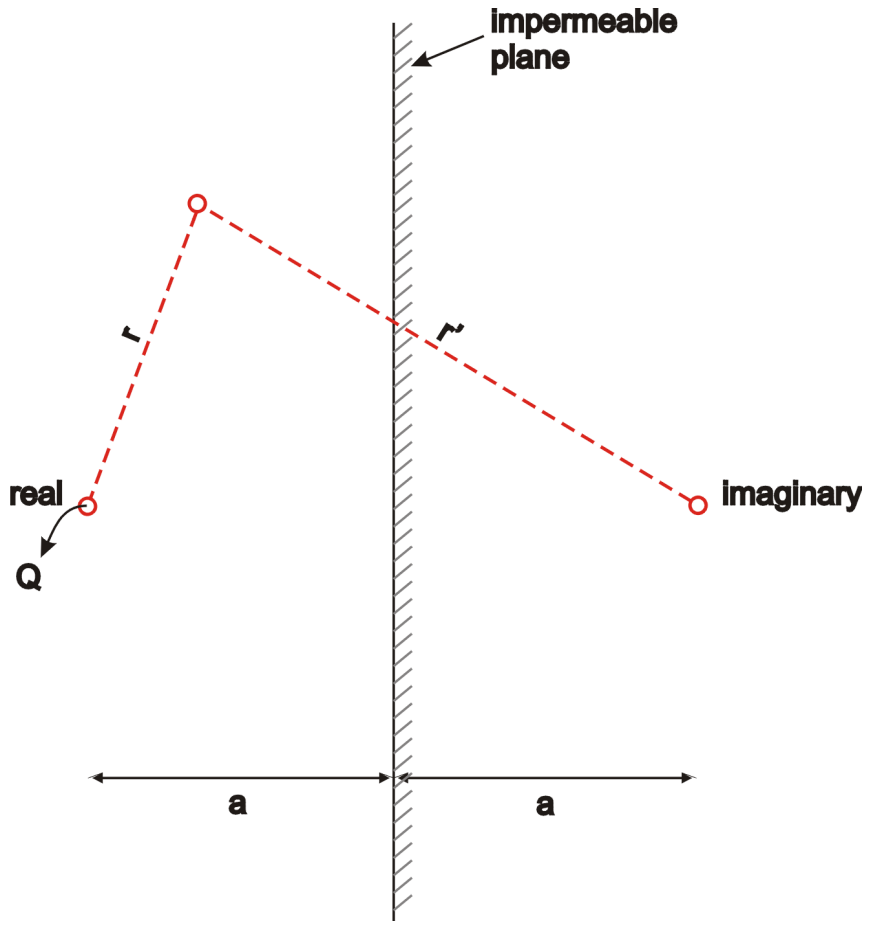

Figure 4. Application of image theory for a single linear impermeable boundary

The drawdown due to the pair of real and imaginary wells is:

$$s = \frac{Q}{4\pi T} W\left(\frac{r^2 S}{4Tt}\right) + \frac{Q}{4\pi T} W\left(\frac{r'^2 S}{4Tt}\right)$$

This solution differs from the solution for a constant-head boundary by the sign on the pumping rate for the imaginary well. Example calculations are shown in Figure 5. When a well is pumped near an impermeable boundary, we observe two intervals of distinct response. During the early period, the observation well responds as if there were no boundary at all. The drawdown steepens after the effects of pumping propagate to the boundary, and the slope on the semilog plot eventually doubles.

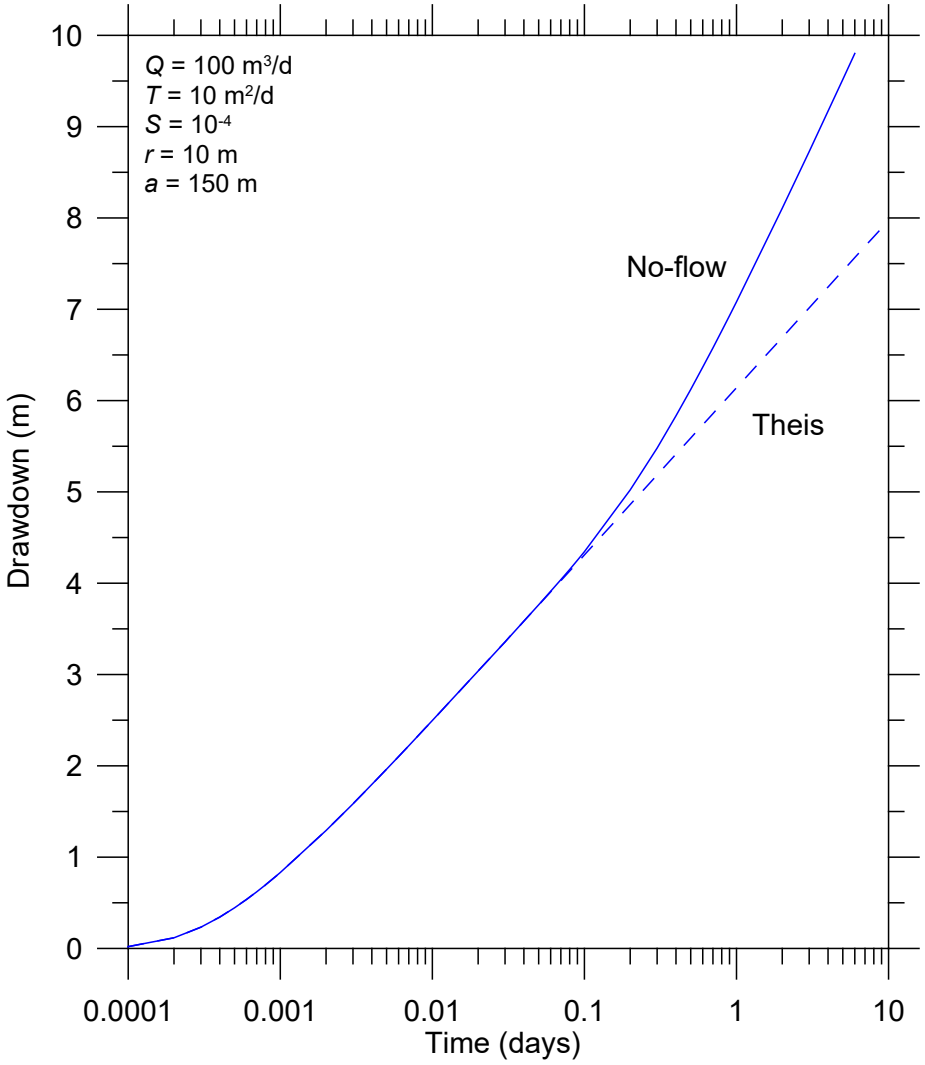

Figure 5. Pumping test in an aquifer with a single linear impermeable boundary

If we use the Cooper-and Jacob (1946) approximation for the Theis well function, the drawdown is given by:

$$s = \frac{Q}{4\pi T}\left[-0.5772 - ln\left\{\frac{r^2 S}{4Tt}\right\}\right] + \frac{Q}{4\pi T}\left[-0.5772 - ln\left\{\frac{r'^2 S}{4Tt}\right\}\right]$$

Using the properties of the log function, this reduces to:

$$\begin{aligned} s &= \frac{Q}{4\pi T} ln\left\{\left[2.2459\frac{Tt}{S}\right]^2 \frac{1}{r^2 r'^2}\right\} \\ &= \frac{Q}{2\pi T} ln\left\{\left[2.2459\frac{Tt}{S}\right]\frac{1}{rr'}\right\} \\ &= \frac{Q}{2\pi T} 2.303\, log_{10}\left\{\left[2.2459\frac{Tt}{S}\right]\frac{t}{rr'}\right\} \end{aligned}$$

Late-time derivative

The derivative of the Cooper-Jacob approximation is given by:

$$\begin{aligned} D_t(s) &= \frac{\partial}{\partial(ln\{t\})}\left[\frac{Q}{2\pi T} ln\left\{\left[2.2459\frac{Tt}{S}\right]\frac{1}{rr'}\right\}\right] \\ &= \frac{Q}{2\pi T} \end{aligned}$$

The derivative of the Cooper-Jacob approximation for an infinite aquifer is given by:

$$D_t(s) = \frac{Q}{4\pi T}$$

We see that the later-time derivative for a linear impermeable boundary is double the derivative for an infinite aquifer.

The doubling of the derivative is diagnostic of the effect of a single linear impermeable boundary. The doubling of the derivative is illustrated in the example calculations shown in Figure 6.

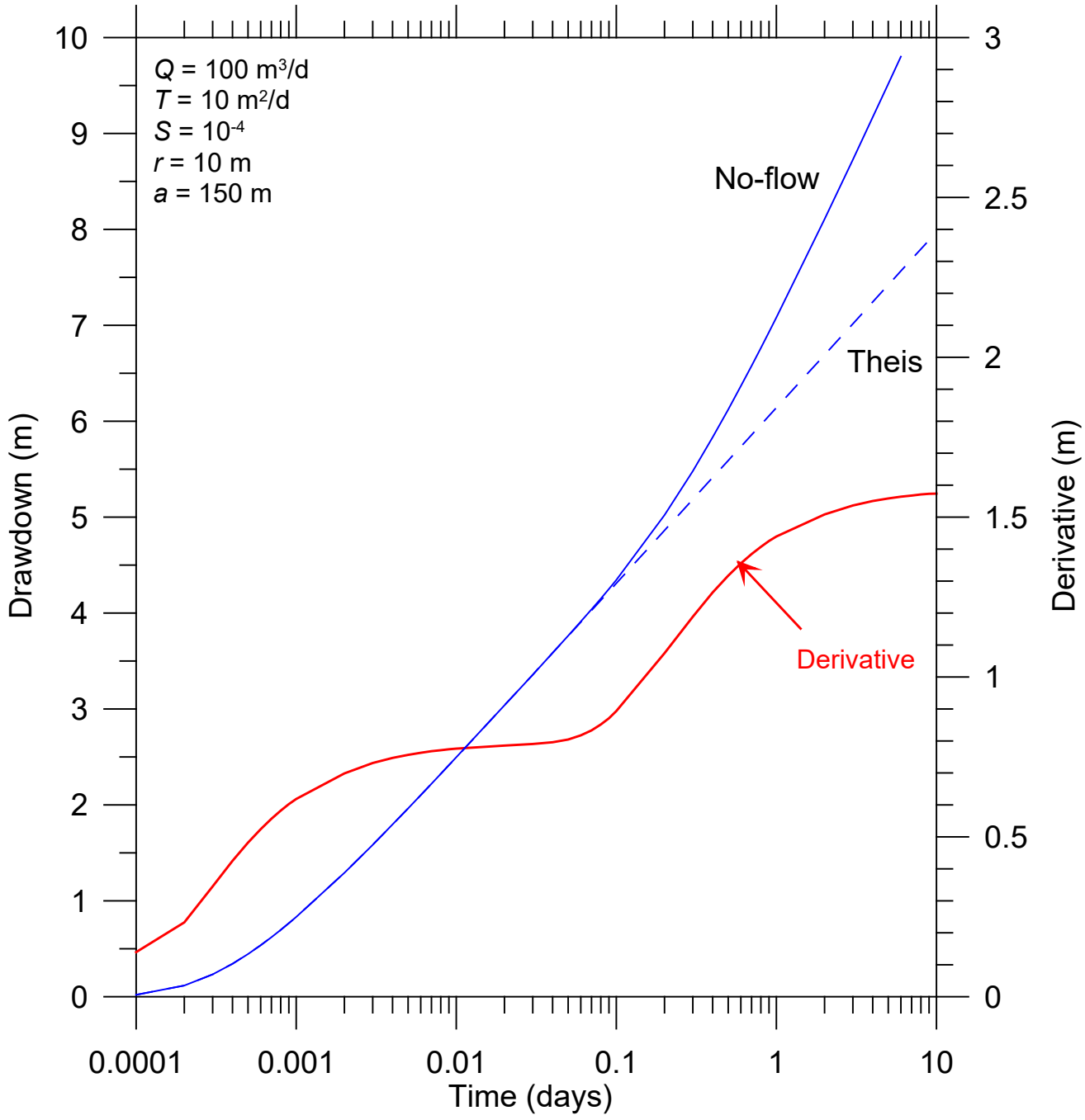

Figure 6. Pumping test in an aquifer with a single linear impermeable boundary

3. Generalization of the results for a single linear boundary

It is unlikely that the connection between a real aquifer and a constant-head feature is perfect or that real boundaries are truly impermeable. The boundaries that we may observe may actually be the interface between the aquifer and regions of relatively higher or lower transmissivity. With respect to interfaces with regions with different properties, the results from the two cases we have examined are important as they effectively bracket the range of responses that may be observed during a pumping test adjacent to a linear boundary:

- *K-Zone 2* >> *K-Zone 1* → Linear constant-head condition; and
- *K-Zone 2* << *K-Zone 1* → Linear no-flow condition.

This concept is illustrated with the results of numerical model simulations. A two-dimensional confined aquifer that is 10 m thick is shown in Figure 7. The model contains two uniform zones. The pumping and observation wells are located in Zone 1 of the aquifer, which is assigned a hydraulic conductivity of 10 m/d. The well pumps at a constant rate of 50 m^3/d. The observation well is located 100 m away, midway to interface with Zone 2.

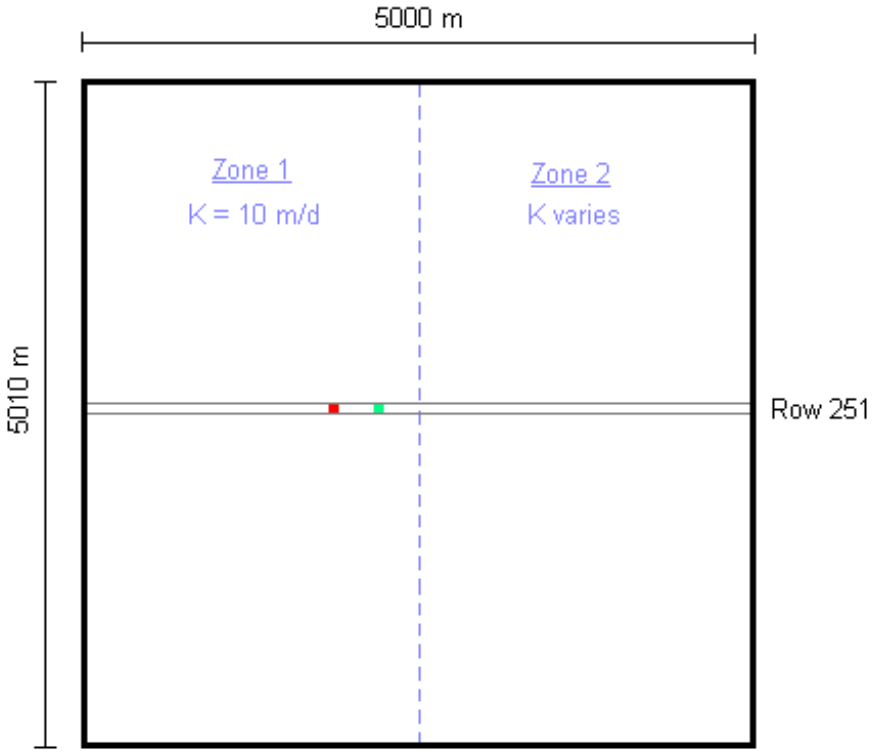

Figure 7. Conceptual model of pumping near a contrast in hydraulic conductivity

The drawdowns at the observation wells are plotted in Figure 8, for hydraulic conductivities of Zone 2 ranging from 1 m/d to 100 m/d. Up to about 0.01 days, the drawdowns are the same for all three cases. This reflects the fact that the effects of pumping are initially contained with Zone 1. After some time, the effects of pumping propagate from Zone 1 to Zone 2, encountering a region with different hydraulic conductivity. The results indicated for K_H = 10 m/d correspond to the "benchmark" results for an aquifer with uniform properties. For a Zone 2 hydraulic conductivity less than 10 m/d, the rate of drawdown increases relative to the benchmark, and for a Zone 2 hydraulic conductivity greater than 10 m/d the rate of drawdown is attenuated.

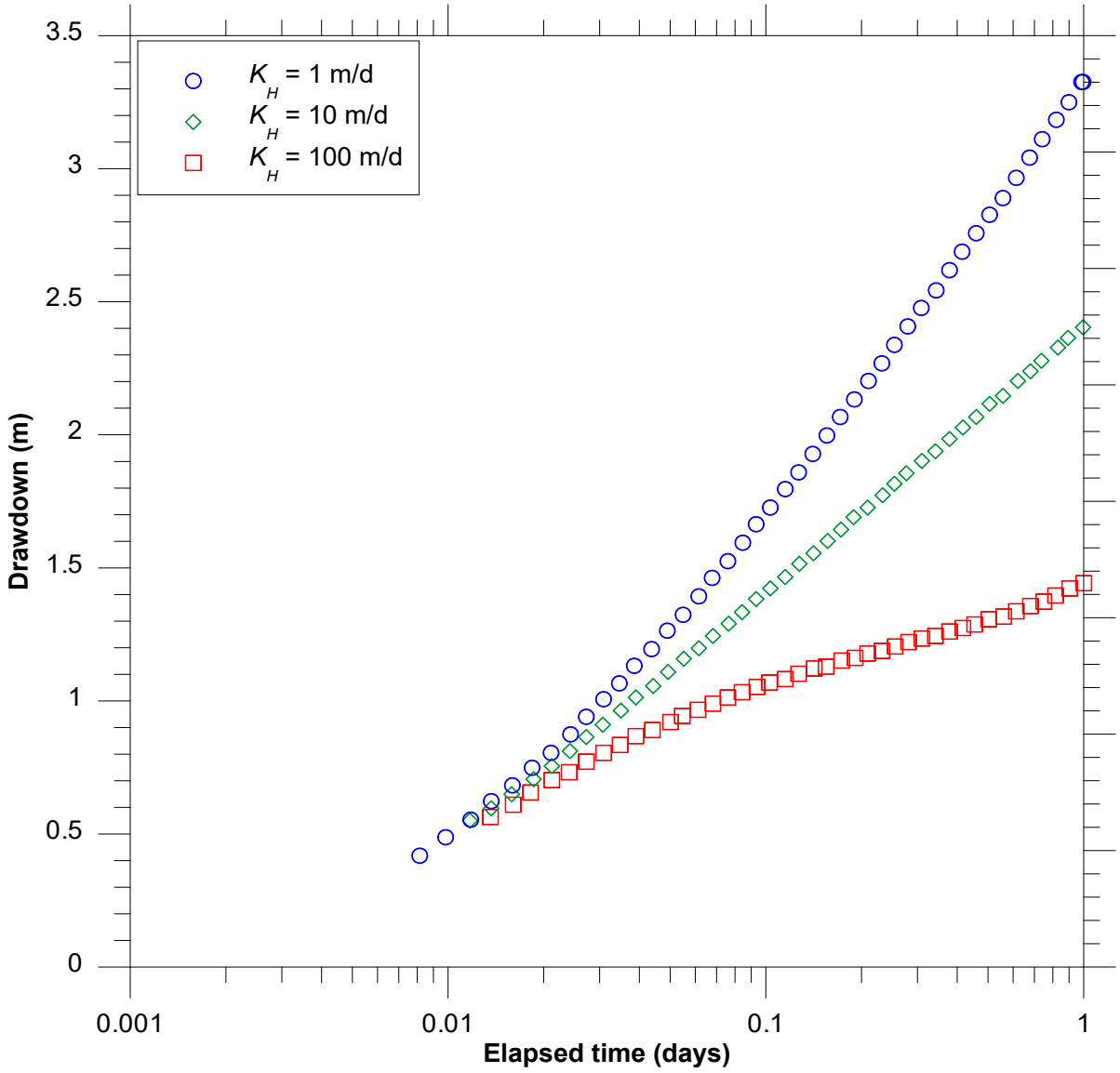

Figure 8. Drawdowns calculated for three values of K_H in Zone 2

To better understand the results of our simulations, we have added the results from analytical solutions with the Theis solution. As shown in Figure 9, the drawdowns for higher conductivities in Zone 2 approach the results obtained with the Theis solution with a single constant-head boundary. The drawdowns for lower conductivities in Zone 2 approach the results obtained with the Theis solution with a single no-flow boundary.

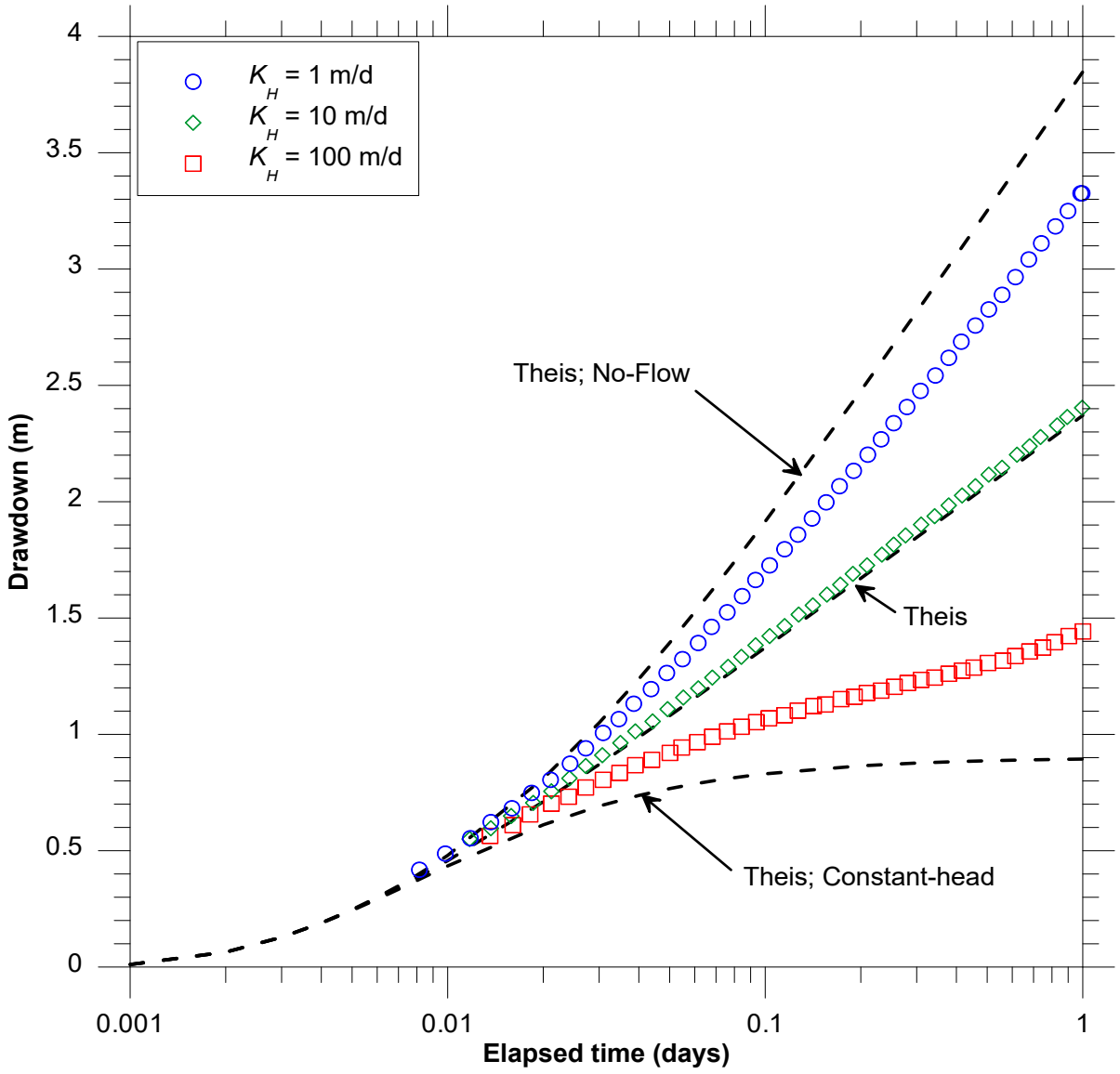

Figure 9. Drawdowns for contrasts in hydraulic conductivity

An expanded view of Figure 9 is shown in Figure 10 with the derivative plots added.

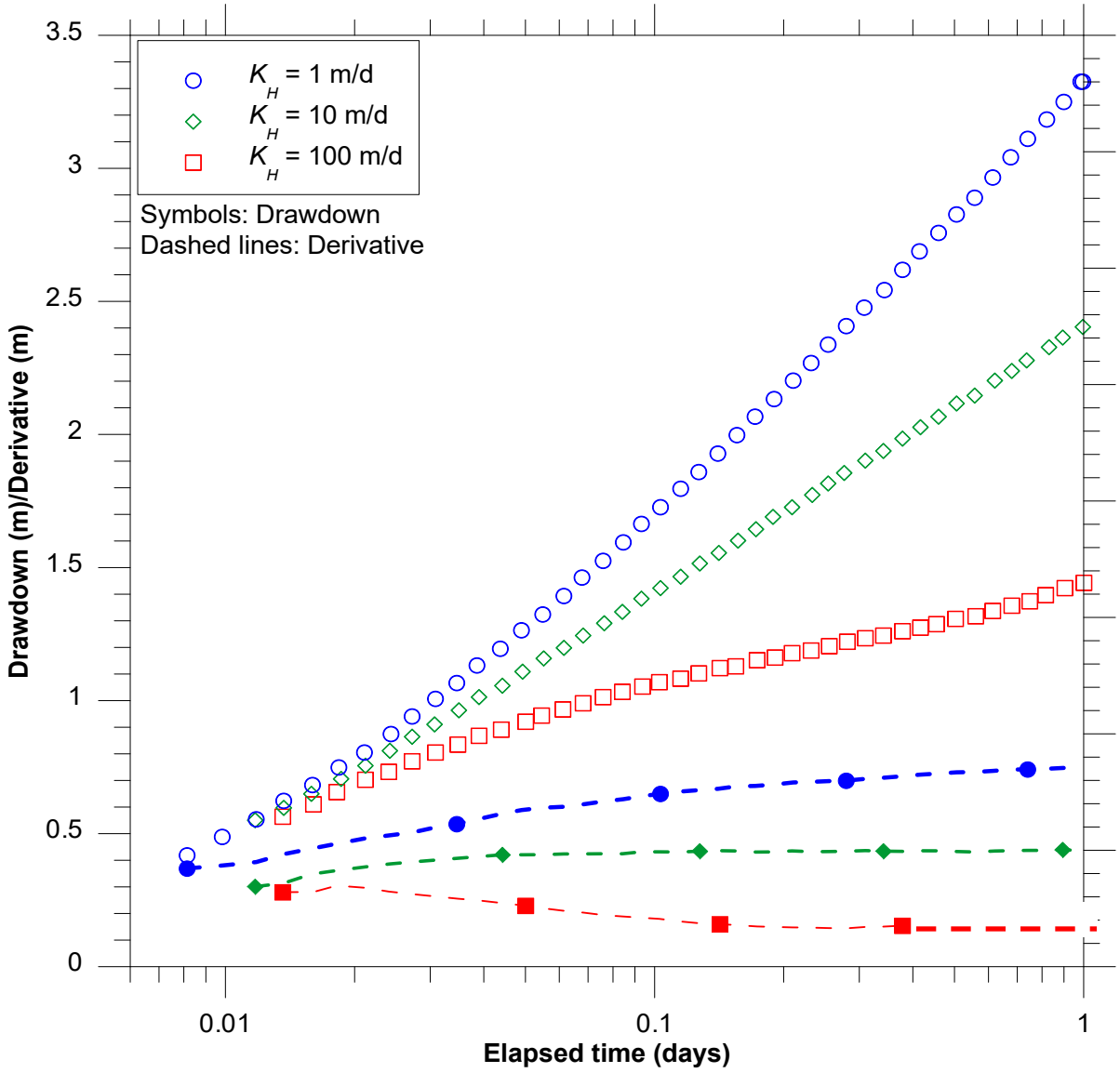

Figure 10. Drawdowns for extreme contrasts in hydraulic conductivity, Derivative plots added

4. Aquifers with two linear impermeable boundaries (channel aquifers)

Buried channel aquifers are important conduits for groundwater in many areas of North America. Preliminary maps of delineated buried channel aquifers in Canada are shown in Figure 10. In western Canada, significant pre-glacial paleochannels have been filled with highly permeable sediments and subsequently overlain by low permeability glacial tills. Buried channel aquifers have been delineated in Alberta (see for example Farvolden, 1963) and Saskatchewan (see for example van der Kamp and Maathuis, 2002). Contrary to what is suggested in Figure 11, studies also suggest that there are buried channel aquifers in Manitoba (Betcher and others, 2005). Buried channel aquifers may also play a significant role in the hydrogeology of southern Ontario (Russell, Hinton, van der Kamp, and Sharpe, 2004).

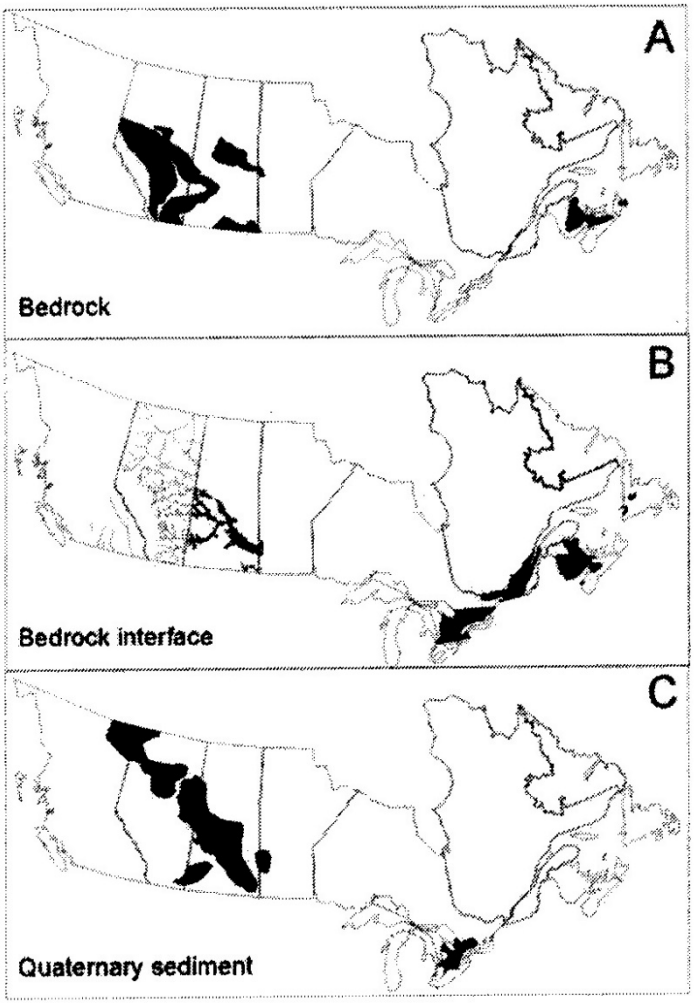

Figure 11. Delineated buried channel aquifers in Canada
(*from* Russell, Hinton, van der Kamp, and Sharpe, 2004)

4.1 Conceptual model for a buried channel aquifer

An essential aspect of buried channel aquifers that controls their response to pumping is the proximity of boundaries. For relatively brief tests, it may be appropriate to ignore the presence of boundaries. This assumption may be too restrictive for channel aquifers. It may limit our analysis to a consideration of drawdowns from only the first few minutes or hours of pumping. The application of an infinite-aquifer analysis does not provide much insight into understanding the effects that boundaries have on the response to pumping, and may provide misleading impressions of the long-term yield of a well.

The idealized conceptual model for a buried channel aquifer is shown in Figure 12. In reality, these aquifers wind their way beneath the present landscape and may have highly heterogeneous distributions of material properties.

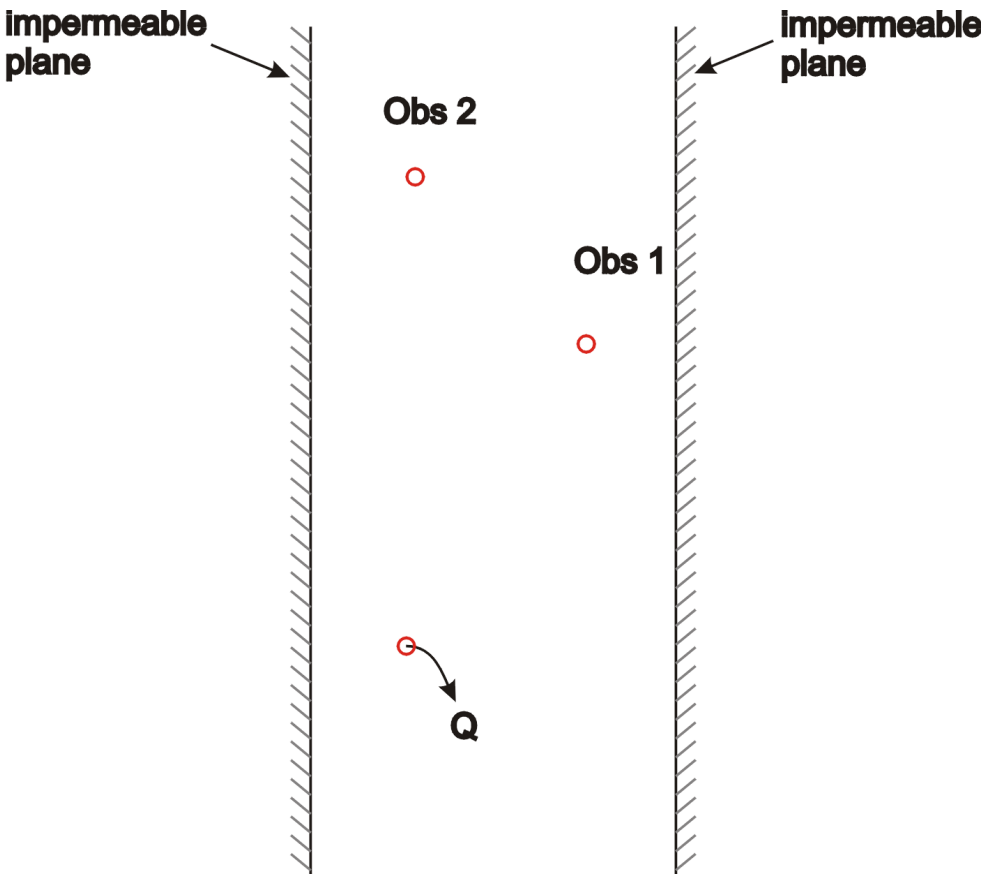

Figure 12. Conceptual model for a buried channel aquifer

An analytical model of a channel aquifer can be assembled using the Theis solution with superposition of image wells. Kruseman and de Ridder (1990; p. 114) present the following formula for pumping between two linear impermeable boundaries:

$$s(r,t) = \frac{Q}{4\pi T}\left[W(u) + \sum_{i=1}^{N} W(A_{ri}^2 u)\right]$$

where *i* through *N* are the image wells. The quantity A_{ri} is defined as:

$$A_{ri} = \frac{r_i}{r}$$

Here *r* is the distance between the real well and the observation well, and r_i is the distance between the image well *i* and the observation well. The set-up of the image wells is shown in Figure 13. The black circle indicates the real well. The white circles indicate the image wells, all of which pump at the same rate as the real well.

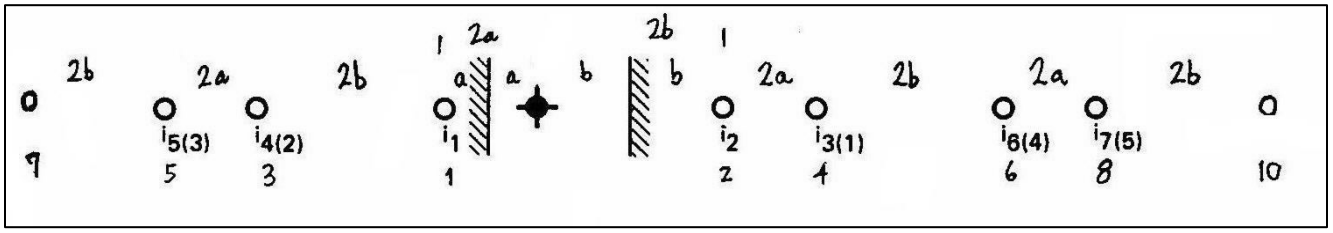

Figure 13. Image well set-up for a buried channel aquifer

Kruseman and De Ridder's formula is presented without a derivation. A good development of the theory of image wells is presented in Ferris and others (1962; p. 144).

In theory, an infinite number of image wells is required. In practice the calculations frequently converge for a relatively small number; however, there may be cases in which many image wells are required to evaluate the solution correctly. The number of image wells required depends on the location of the observation well and the elapsed time, and, in my experience, there is no easy way to anticipate how much computational effort is appropriate. A convergence analysis is generally required, in which the number of image wells is increased until the addition of another image well has negligible effect on the calculated drawdowns.

Vandenburg (1977) and Motz (1991) developed type curves for the interpretation of pumping tests in channel aquifers. van der Kamp and Maathuis (2002) demonstrated the application of these type curves in the context of a case study in Saskatchewan. The capability to interpret tests in channel aquifers is incorporated in AQTESOLV (versions Version 3.71.003 and later). The results of benchmark analyses are presented here to check the implementation of this capability and to develop our intuition regarding the responses to pumping in buried channel aquifers.

4.2 Benchmark analysis for pumping from a buried channel aquifer

Benchmark results are calculated using the finite-difference simulation code MODFLOW. We consider a perfectly confined aquifer with uniform thickness, and uniform, isotropic transmissivity. The aquifer is relatively long and thin, and is truncated along its left and right by impermeable boundaries. The conceptual model for the problem is shown in Figure 14.

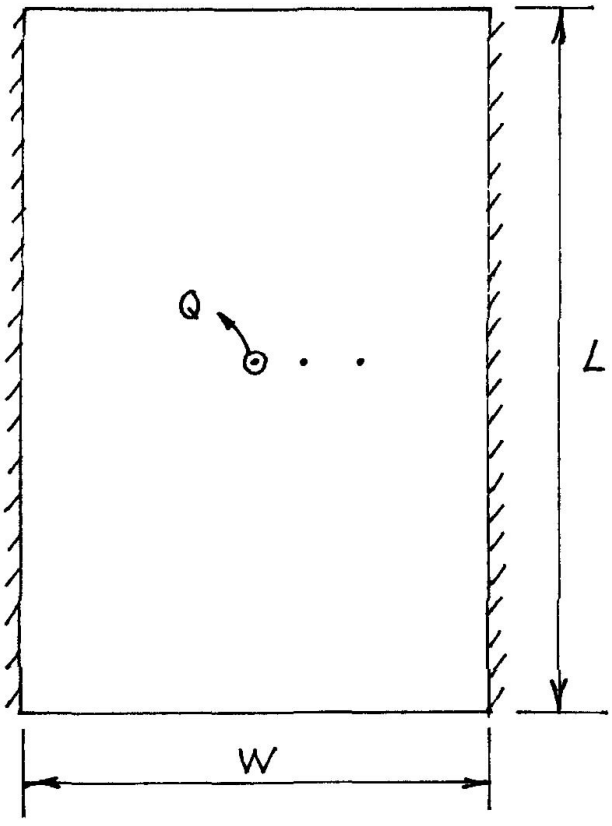

Figure 14. Schematic of MODFLOW model of a buried channel aquifer

Parameters

- Aquifer width, $W = 510$ m
- Transmissivity, $T = 8.64$ m^2/day (medium sand, $K_H = 10^{-3}$ cm/sec, $B = 10$ m)
- Storativity, $S = 10^{-4}$
- Pumping rate, $Q = 109.02$ m^3/day (20 US gpm)

The coordinates of the wells are listed below.

Well	*x*-coordinate (m)	*y*-coordinate (m)
PW-1	0.0	0.0
OW-1	20.0	0.0
OW-2	50.0	0.0

MODFLOW model

- A single model layer is used to represent the aquifer with an arbitrary thickness of 1.0 m;
- The model is discretized with 51 columns across its width, with a uniform spacing of 10.0 m;
- By necessity, the model must also be truncated along its north and south boundaries. The aquifer is 2000 m long, and is discretized with 200 rows along its length, with a uniform spacing of 10.0 m; and
- The duration of the simulation is 10 days. A single stress period is divided into 200 time steps, with a time-step multiplier of 1.1.

The analytical solution that we will compare with the MODFLOW results is based on the assumption that the aquifer is infinitely long. In this example, the duration of pumping is sufficiently long that the effects of pumping extend to the north and south boundaries of the model, violating this assumption. To assess the boundary effects, two numerical simulations are conducted with different boundary conditions along the north and south boundaries of the model:

- Analysis #1: Constant-head conditions; and
- Analysis #2: No-flow conditions.

Results for constant-head conditions along the north and south boundaries

The results for constant-head conditions along the north and south model boundaries of the MODFLOW model are shown in Figure 15. The match between AQTESOLV and the MODFLOW results is excellent. A comparison of the two sets of results suggests that the north and south boundaries manifest themselves after about 3 days of pumping. As expected, the drawdowns calculated with the numerical model eventually decline below the analytical solution.

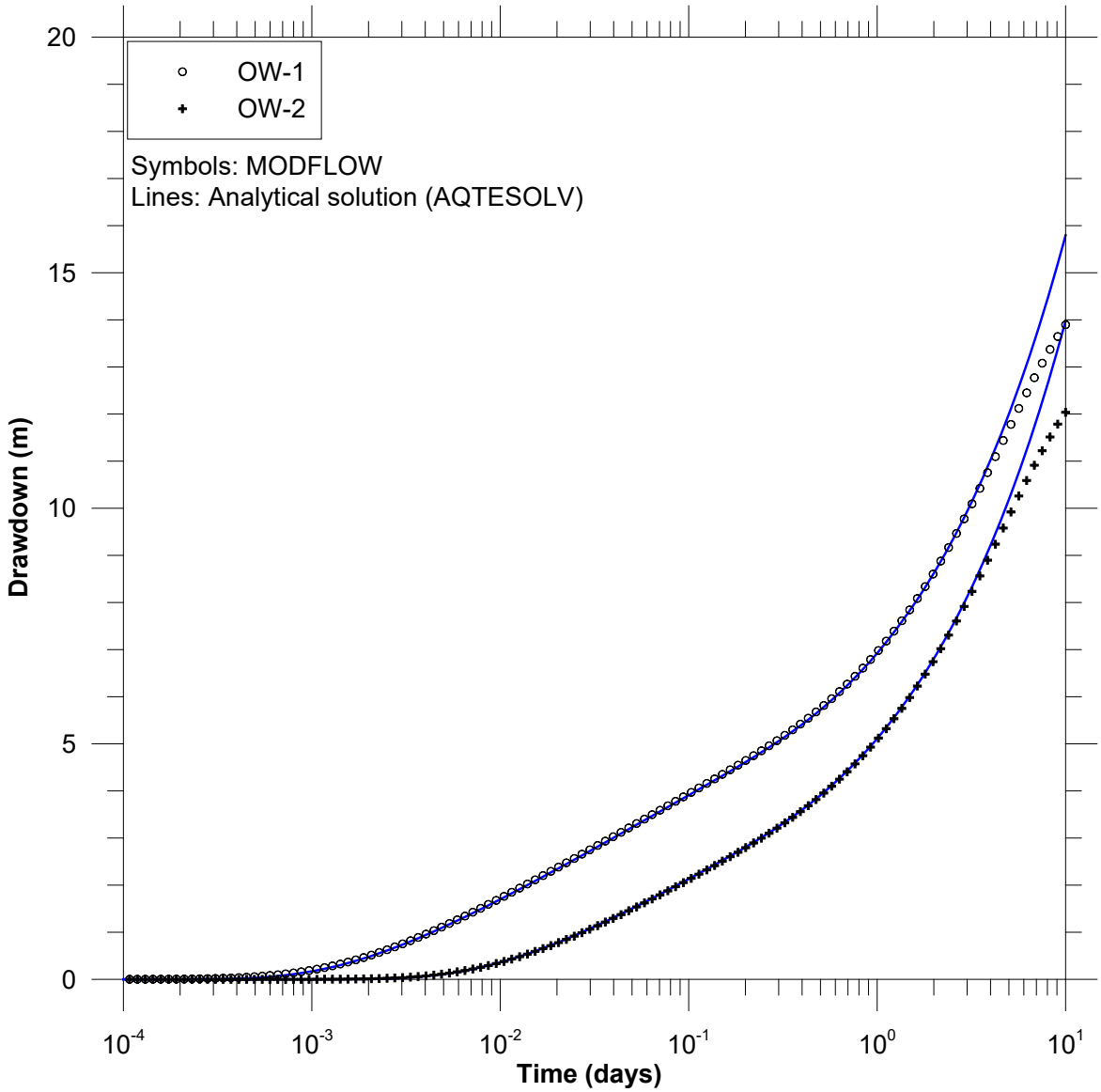

Figure 15. Comparison of drawdowns, constant-head conditions

Results for no-flow conditions along the north and south boundaries

The results for no-flow conditions along the north and south model boundaries of the MODFLOW model are shown in Figure 16. The match between AQTESOLV and the MODFLOW results is again excellent. A comparison of the two sets of results suggests that the influence of the north and south boundaries is detected about 3 days of pumping. Beyond that time, the drawdowns calculated with the numerical model exceed those predicted by the analytical solution.

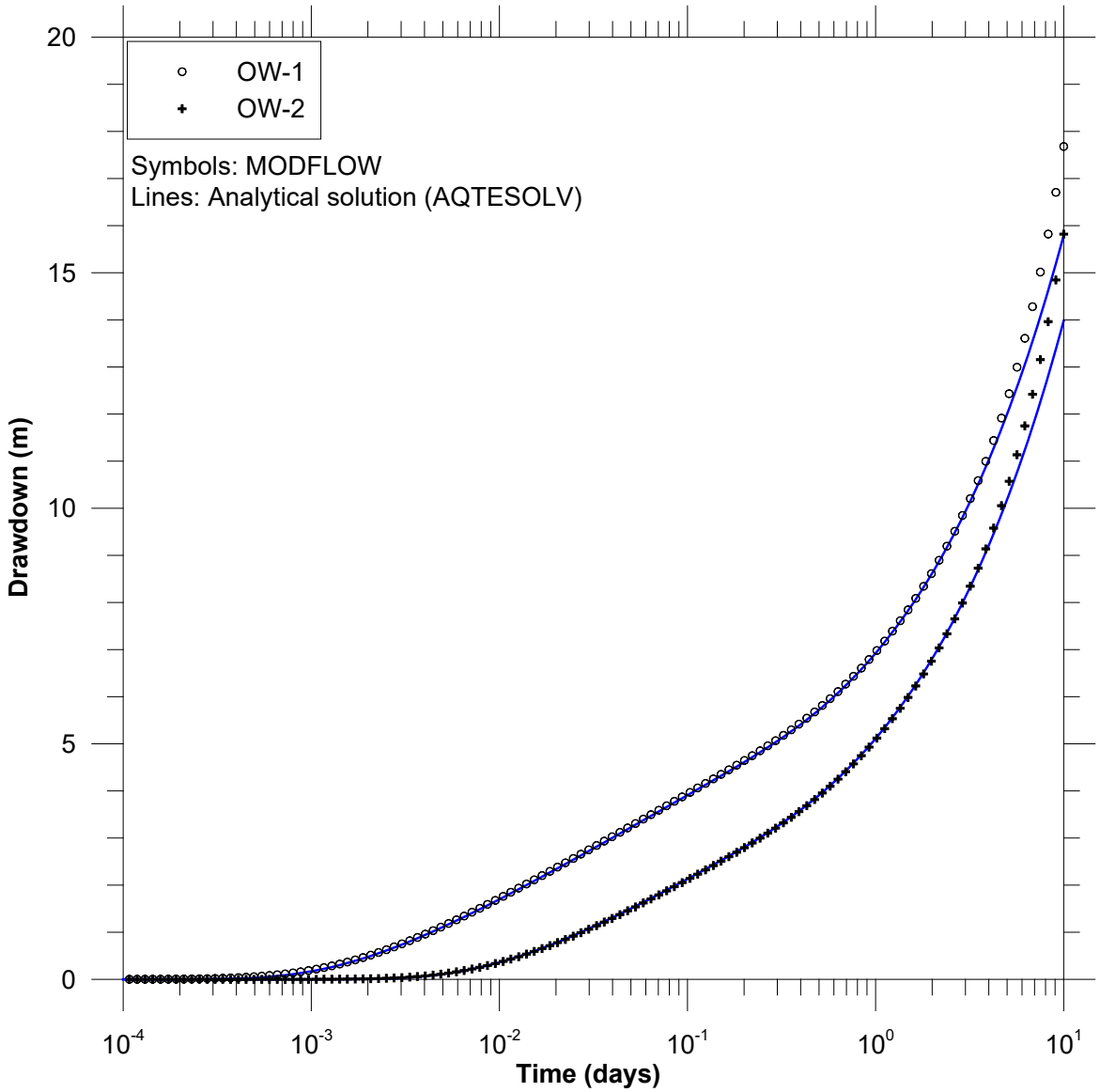

Figure 16. Comparison of drawdowns, no-flow conditions

4.3 Diagnostic plots for buried channel aquifers

The most appropriate way to diagnose the response to pumping in a channel aquifer is with separate plotting approaches for early and late time, including the derivative plots. A semi-log diagnostic plot for the early time response for OW-1 is shown in Figure 17. The semi-log straight line plot of the drawdown and the plateau of the derivative are characteristic of the infinite aquifer response that precedes the drawdown cone expanding to the boundaries. The derivative increases rapidly beyond the departure from the infinite-aquifer response and shows no sign of stabilizing. These results demonstrate that the presence of two linear no-flow boundaries causes more than a simple doubling of the slope on a semilog plot.

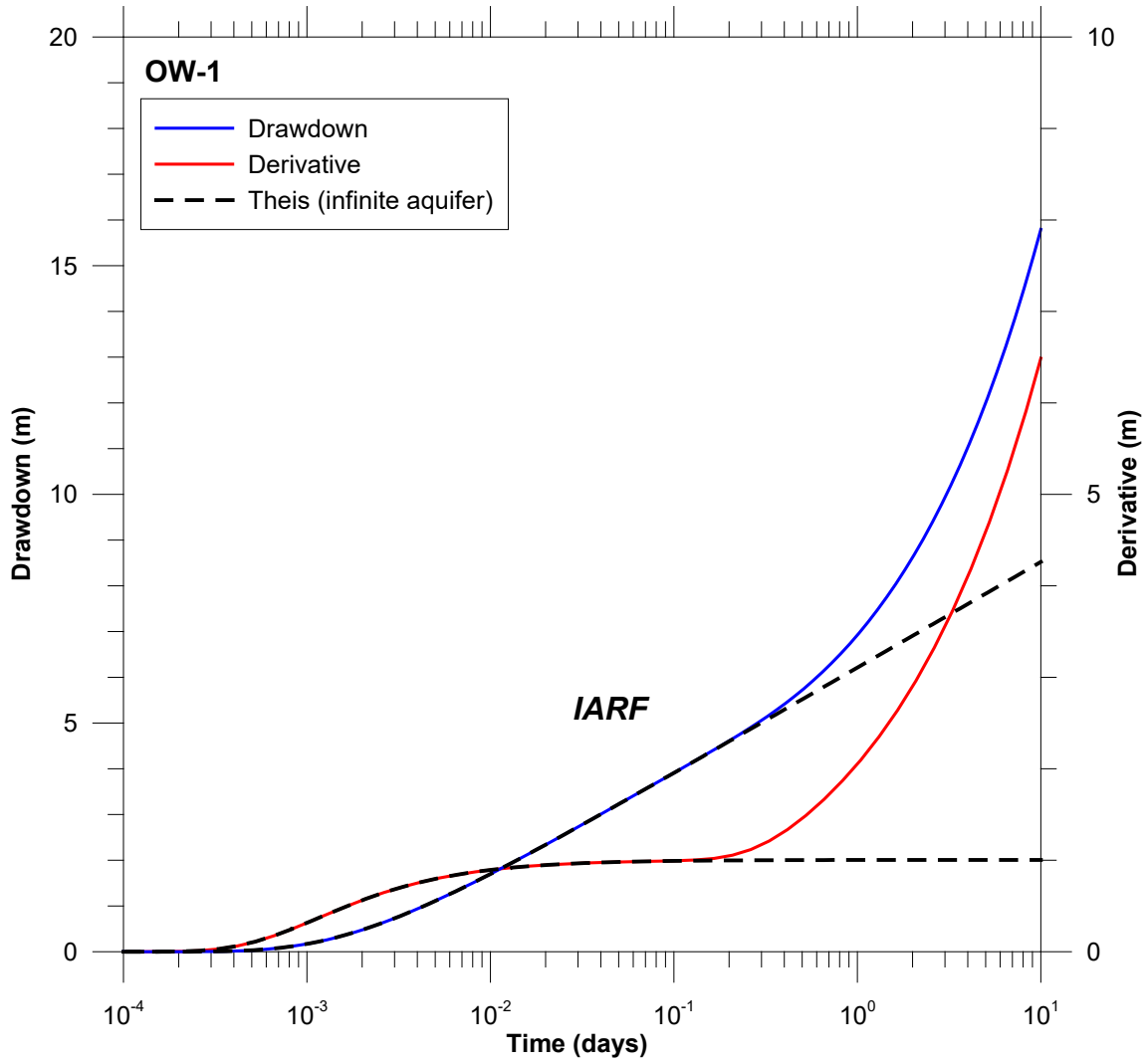

Figure 17. Drawdown and derivative plots for the analytical solution

Another way to look at the response for OW-1 is shown in Figure 18. In this figure, the drawdowns and derivatives for the analytical solution are plotted on log-log axes. This alternative form provides two more diagnostic suggestions of a channel aquifer. For later times, the drawdown and derivative plot as straight lines on log-log axes. The late-time slope of the drawdown is 1 log cycle of drawdown vs. 2 log cycles of time. This slope is characteristic of a linear flow regime.

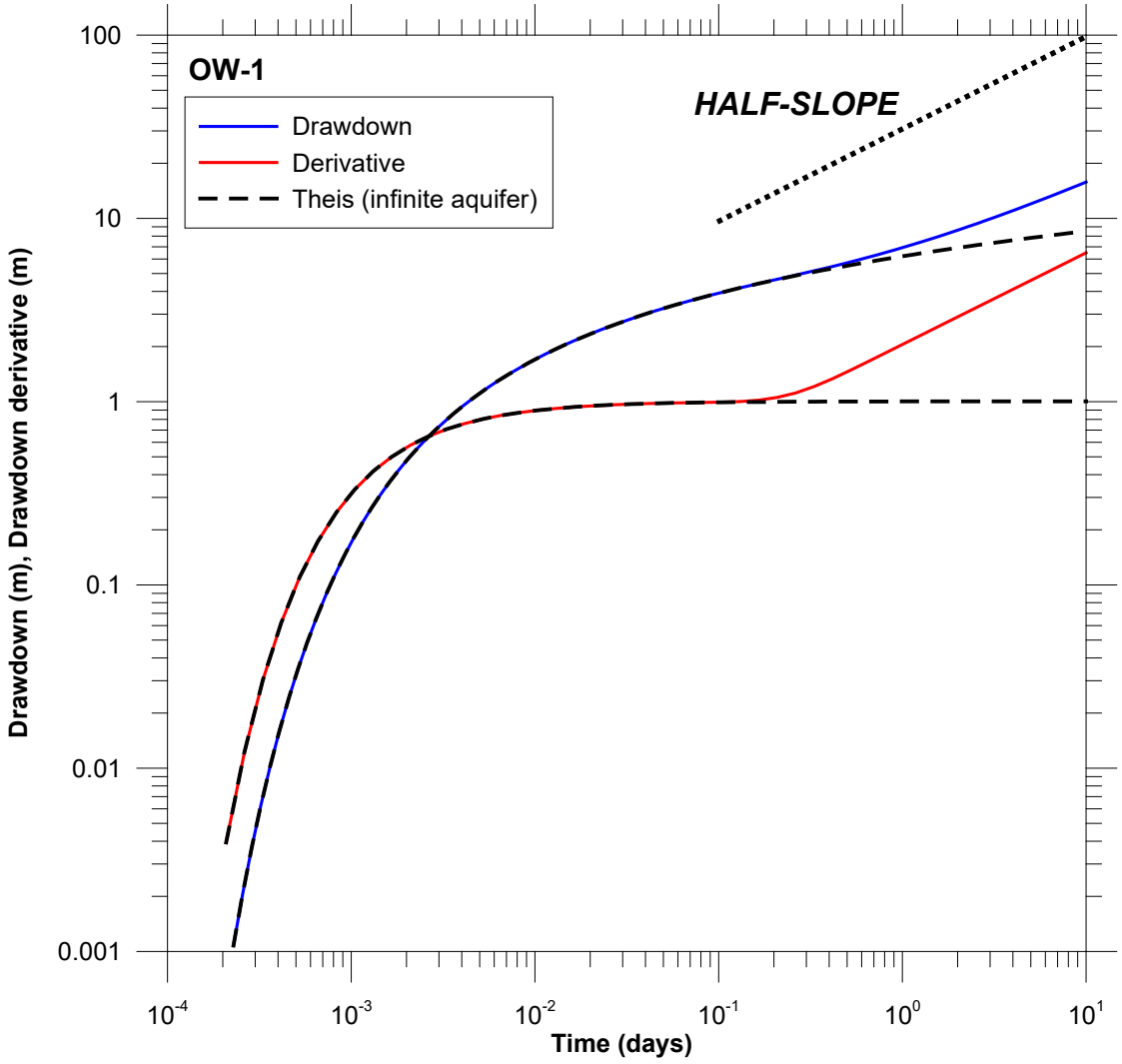

Figure 18. Drawdown and derivative plots for the analytical solution: log-log axes

5. Case study: Estevan, Saskatchewan

In March 1965, the Saskatchewan Research Council conducted a pumping test in an aquifer about 13 miles northwest of Estevan, Saskatchewan. In this case study, we revisit the original analysis of the pumping test presented in Walton (1970). The original analysis made use of data from the first few minutes of a long-term test. The data are re-examined using composite plots and derivative analysis. A re-analysis of the complete data set is conducted using an analytical approach for channel aquifers that incorporates the effects of the boundaries.

The aquifer is a long, sinuous paleochannel infilled with permeable sand and gravel and overlain by about 150 m of low-permeability glacial till. The geologic data available at the time of the pumping test suggested that the aquifer was a strip of sand and gravel approximately 1,700 feet wide, trending north-northwest through the production well. Descriptions of the hydrogeology of the Estevan area and the responses to pumping are presented in the excellent papers of van der Kamp and Maathuis (2002) and Maathuis and van der Kamp (2003).

The location of the pumping test site is shown in Figure 19. The generalized stratigraphic logs and construction features of the wells are shown in Figure 20. The wells were all screened in approximately the same depth intervals and are open to the coarse sand and gravel materials near the base of the glacial deposits. Johnson stainless steel continuous-slot screens were installed at selected depth intervals.

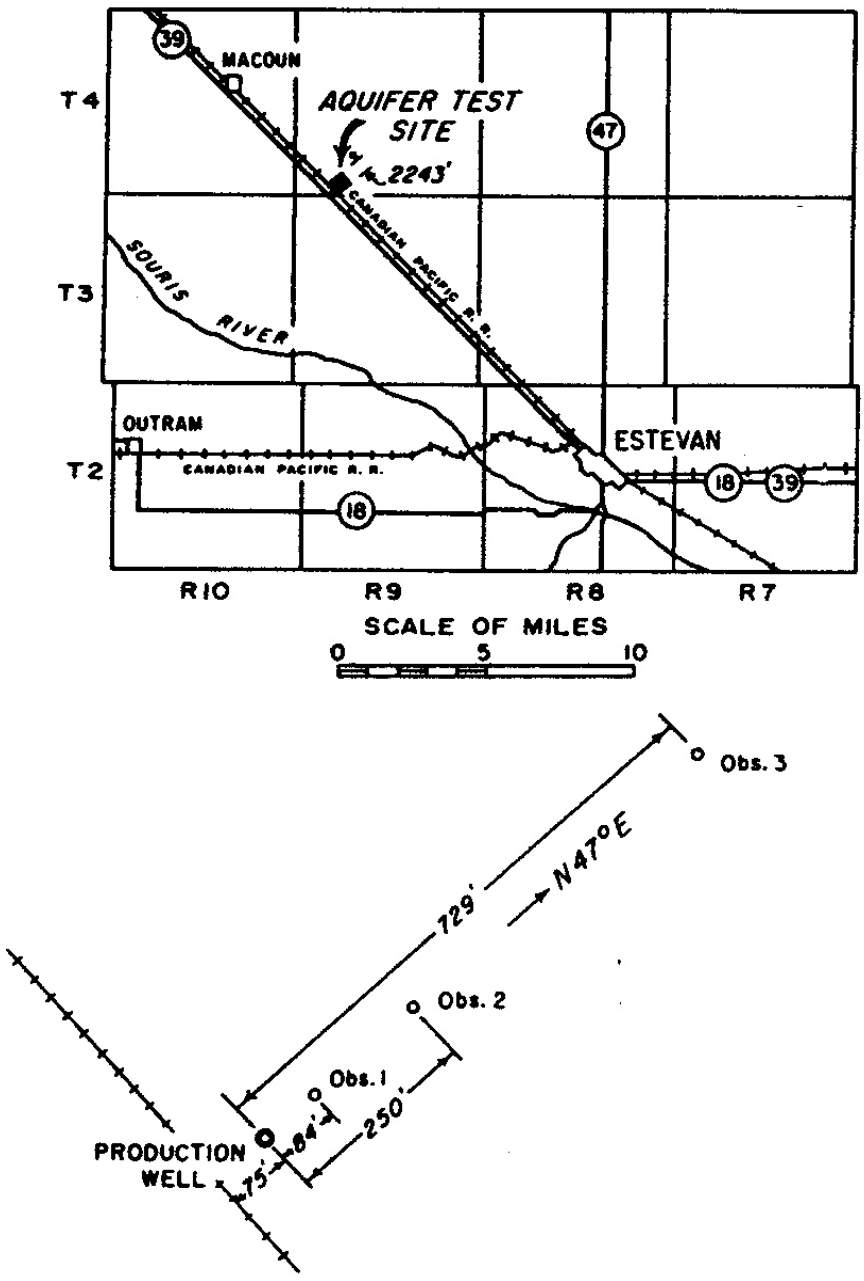

Figure 19. Locations of wells monitored during Estevan pumping test
Reproduced from Walton (1970)

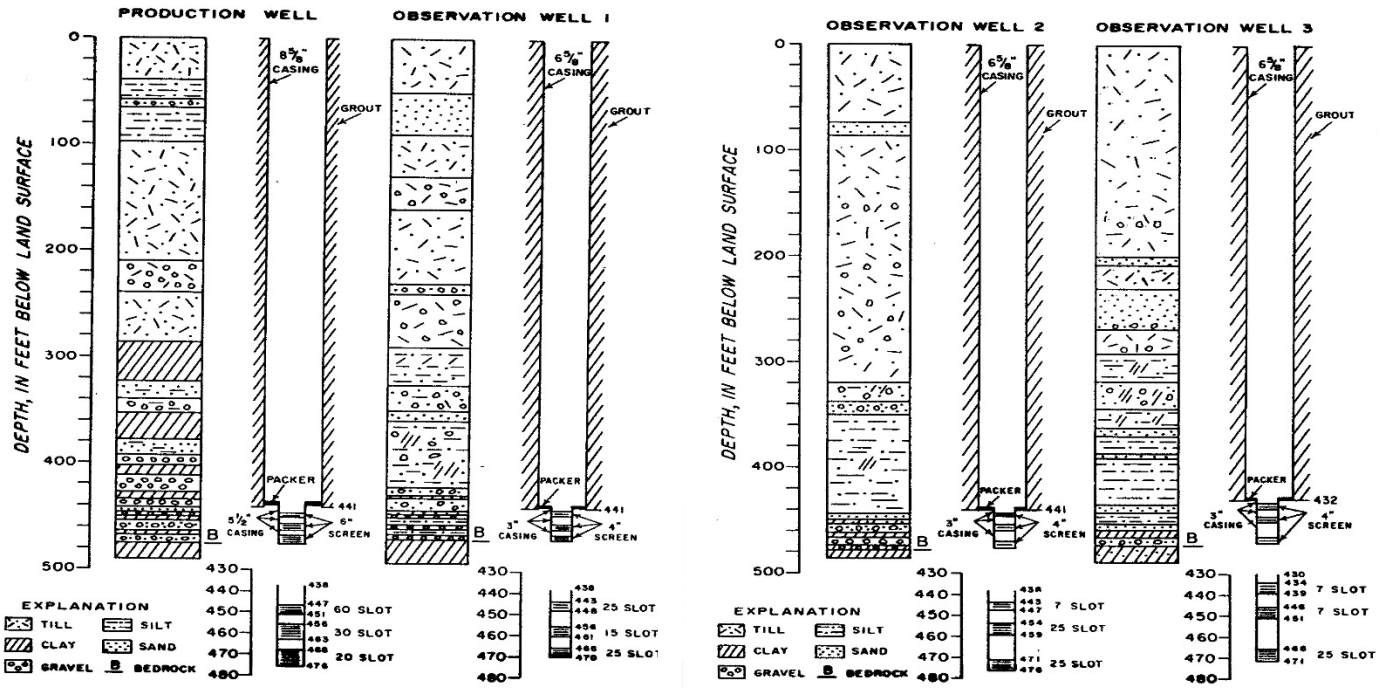

Figure 20. Geologic logs and completion details for wells
Reproduced from Walton (1970)

Pumping test data

Pumping started at 3:00 PM on March 4 and continued at a constant rate of 460 Igpm until 2:00 PM on March 12. The duration of pumping was 11,520 minutes. The pumping rate was held constant by means of a gate valve installed in the discharge pipe. A circular orifice and a manometer tube installed in the end of the discharge pipe were used to measure the rate of pumping. The rate of pumping varied between 457 Igpm and 464 Igpm.

Water levels were measured at the production well and at three observation wells. Water levels in the production well were frequently measured with a steel tape; water levels in the observation wells were continuously measured by means of recording gages. Atmospheric-pressure changes were measured with a recording Belfort microbarometer.

Drawdowns in the wells were determined by comparing water levels measured before pumping started with water levels measured during the pumping period. The drawdowns were corrected for changes in atmospheric pressure. The drawdowns in the wells at the end of the test are tabulated below.

Well	Drawdown at end of test (ft)
Production well	16.03
Observation well 1	10.97
Observation well 2	10.88
Observation well 3	9.54

A drawdown of 0.59 foot was observed in well GSC-3A which penetrated the lower aquifer about 9 miles northeast of the production well. This drawdown indicates that cones of depression under heavy pumping conditions may spread to great distances.

Original analysis (Walton, 1970)

Walton remarked that observation wells 1 and 2 were close to the pumped well and their time-drawdown curves were relatively flat. Analysis of the time-drawdown curves for these wells was most difficult and emphasis was placed on the time-drawdown graph for observation well 3 in determining *T* and *S*. The original analysis of Walton (1970) for observation well 3 is reproduced in Figure 21.

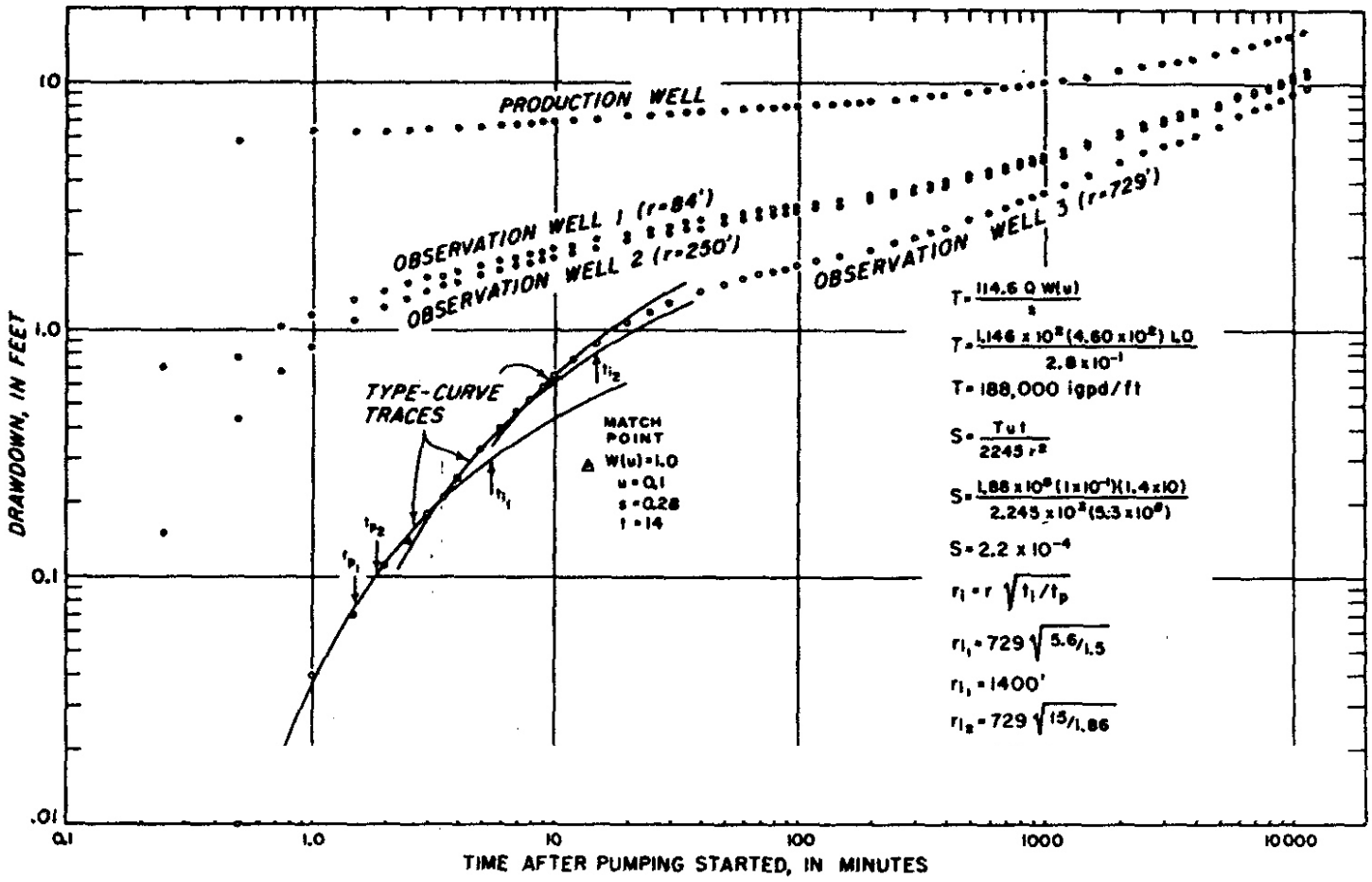

Figure 21. Original analysis
Reproduced from Walton (1970)

Walton interpreted the test data using the Theis type-curve matching method. As shown in Figure 21, Walton matched the type curve to early time-drawdown data. The coordinates of the match point are:

- $u = 0.1$;
- $W(u) = 1.0$;
- $t = 14$ min; and
- $s = 0.28$ ft.

The type curve matching yielded a transmissivity of 188,000 Igpd/ft (30,220 ft^2/day) and storativity of 0.00022, respectively. According to Walton, the transmissivity is very high and the storage coefficient is in the normal range for a confined aquifer.

After about 3 minutes of pumping, the time-rate of drawdown in the observation wells increased and field data deviated upward from the type-curve trace, indicating the presence of a barrier boundary. The type curve was again matched to drawdown data for time values between 3.5 and 8.0 minutes. After about 8 minutes, the time-rate of drawdown again increased, indicating the presence of a second barrier boundary. The type curve was again matched to drawdown data for time vales between 8 and 15 minutes. The divergence of the three type-curve traces was determined and the distances from the observation wells to image wells associated with the two barrier boundaries were calculated.

We object to several aspects of Walton's original analysis. There are at least four reasons why we cannot place much reliability in the transmissivity estimated in the original analysis:

- The analysis ignored essential aspects of the site. Walton (1970) describes these aspects clearly but they are not incorporated in the analysis;
- The analysis was conducted on a well-by-well basis;
- The analysis focused on only the very earliest portion of the test. For observation well #3, the transmissivity was estimated based on data from only the first 3 minutes of a test that lasted more than 10,000 minutes; and
- No attempt is made to diagnose the response to pumping or to interpret the data with an analysis that incorporates the conceptual model for this site.

Alternative analyses

Diagnostic plots

A log-log plot of the drawdowns is presented in Figure 22. This is the key plot for identifying that we are pumping from a buried channel aquifer. As shown in the plot, towards the end of the test the drawdowns appear to approximate straight lines with a half slope (one log cycle of drawdown per two log cycles of time). The half-slope is characteristic of linear flow in a channel aquifer.

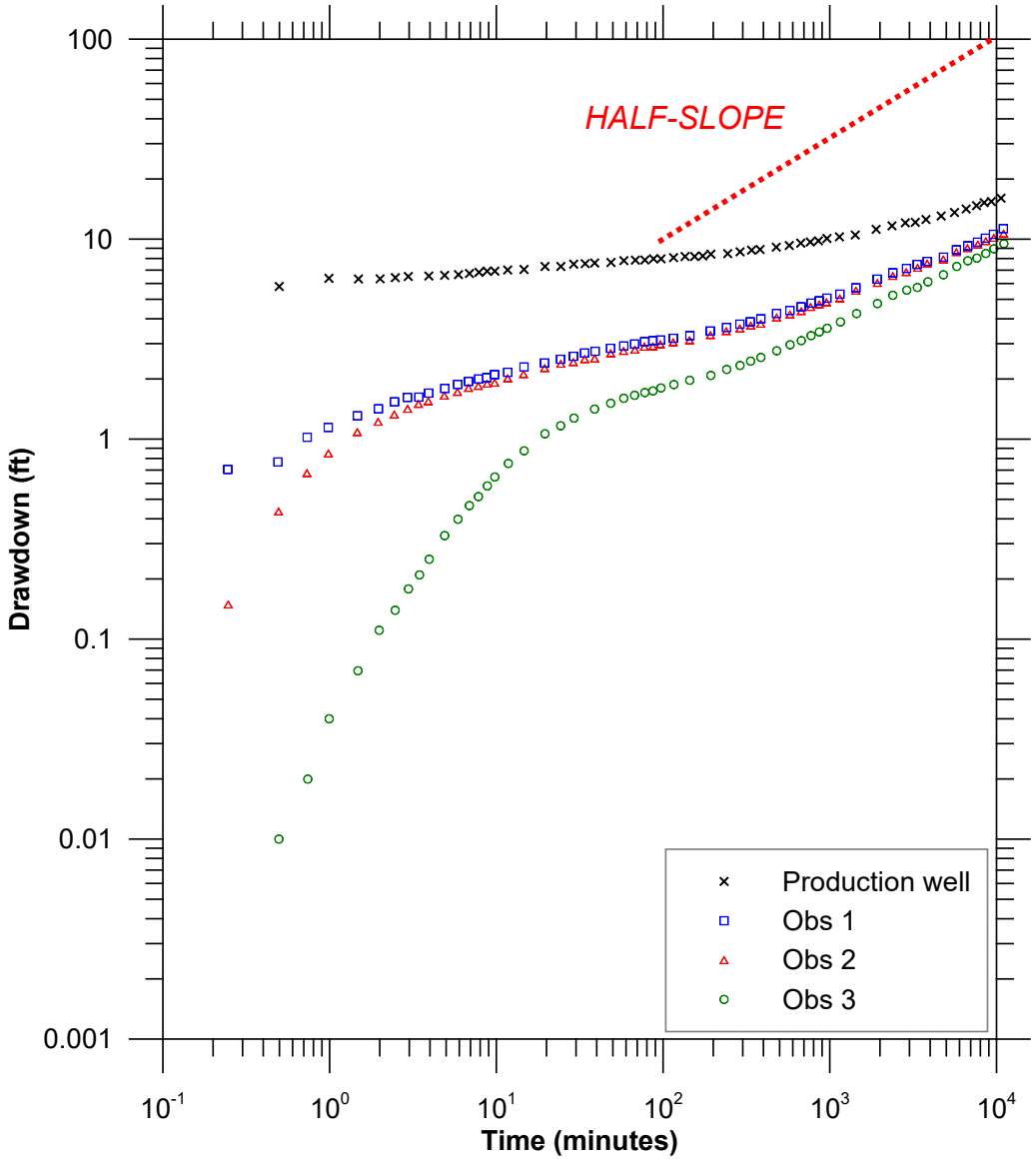

Figure 22. Time-drawdown records on a log-log plot

The derivatives are plotted on log-log axes in Figure 23. The theoretical late-time derivative for a channel aquifer also has a half-slope of a log-log plot, and this is clearly evident in the Estevan data.

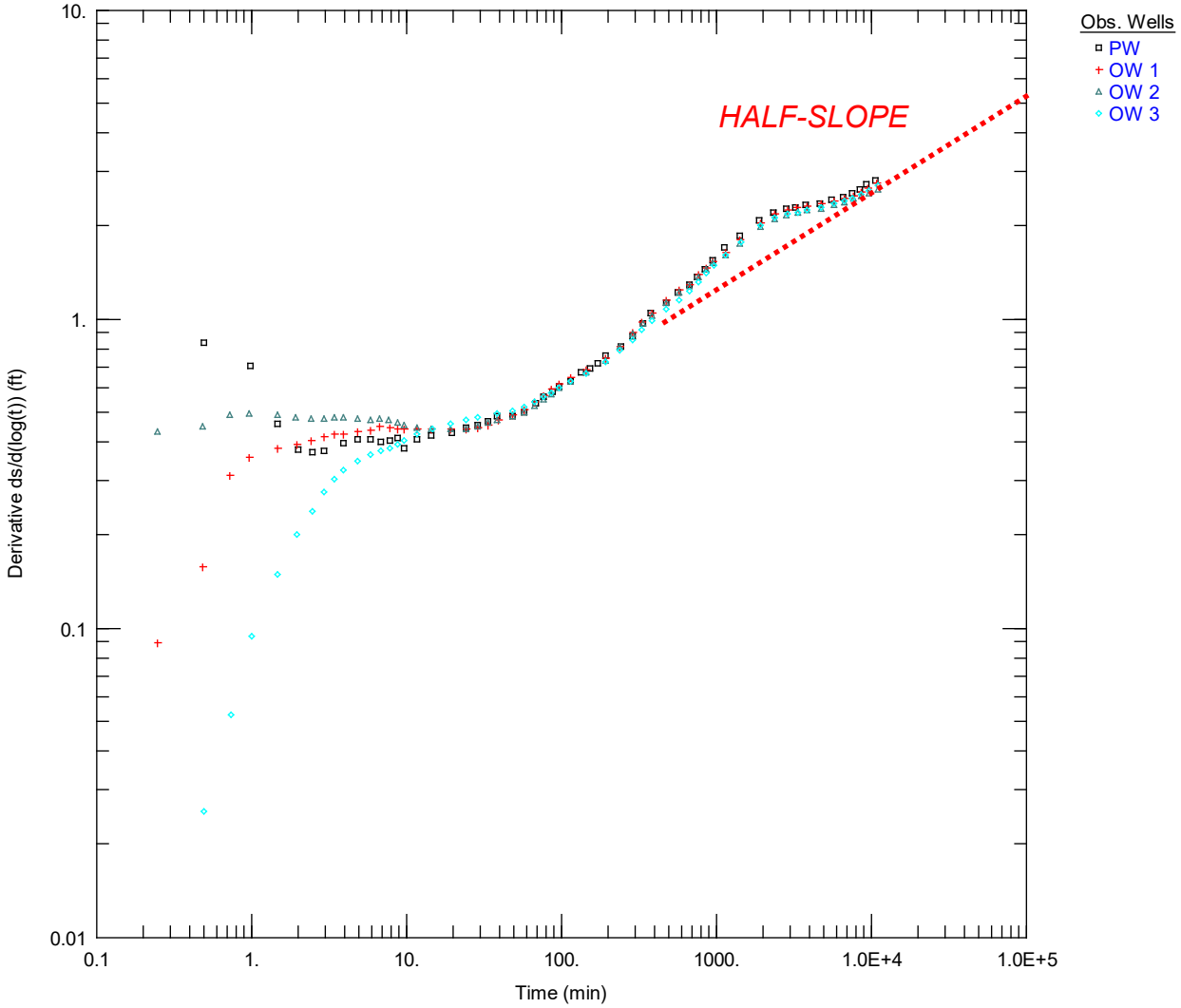

Figure 23. Derivative plot on log-log axes

To estimate the bulk-average transmissivity we assemble the drawdowns on a semilog composite plot. The original drawdown data from all of the wells are re-plotted in Figure 24, with the abscissa being elapsed time divided by the square of the distance from the production well (t/r^2). This plot is in effect a diagnostic plot for the early-time, infinite-aquifer response.

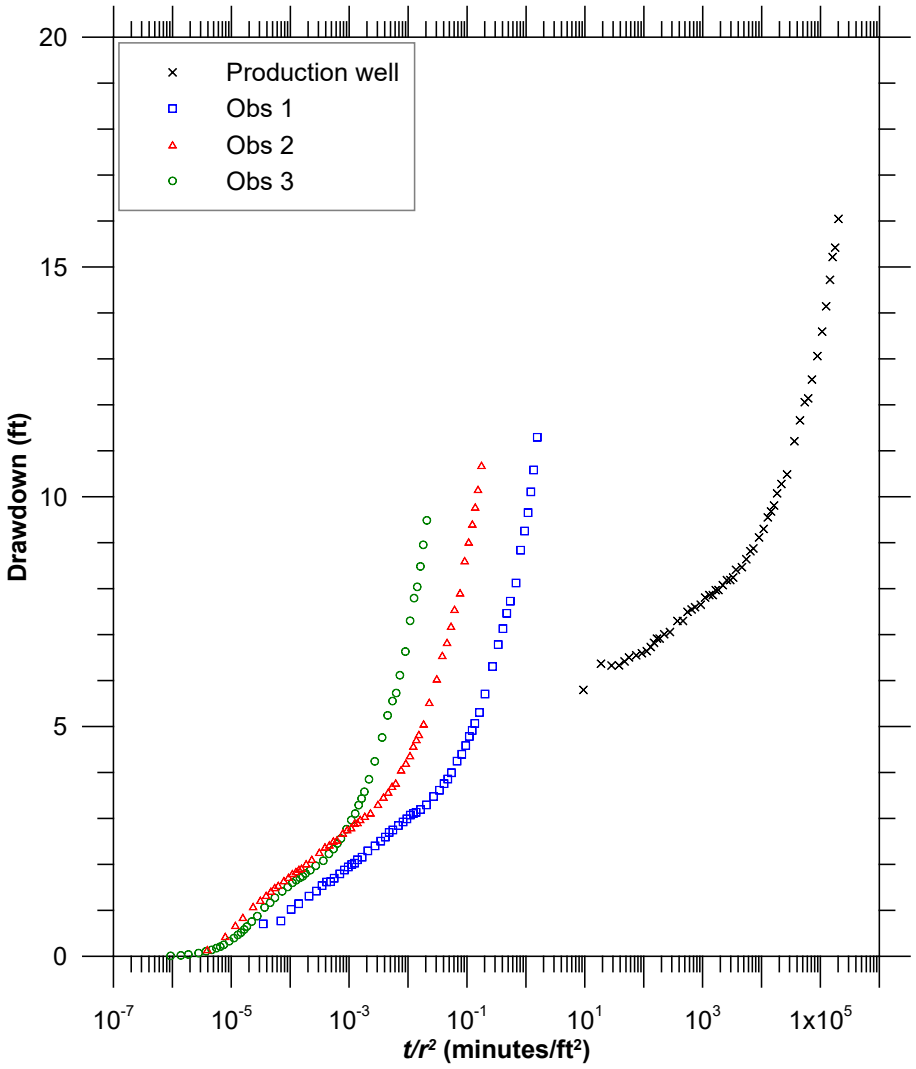

Figure 24. Semilog composite plot

The early portions of the responses from all wells, including the production well, appear to converge on parallel straight lines on the semi-log composite plot shown in Figure 24. The parallel straight lines superimposed on the data in Figure 25 represent the combination of values of t/r^2 over which the aquifer responds as a perfectly confined aquifer of infinite extent.

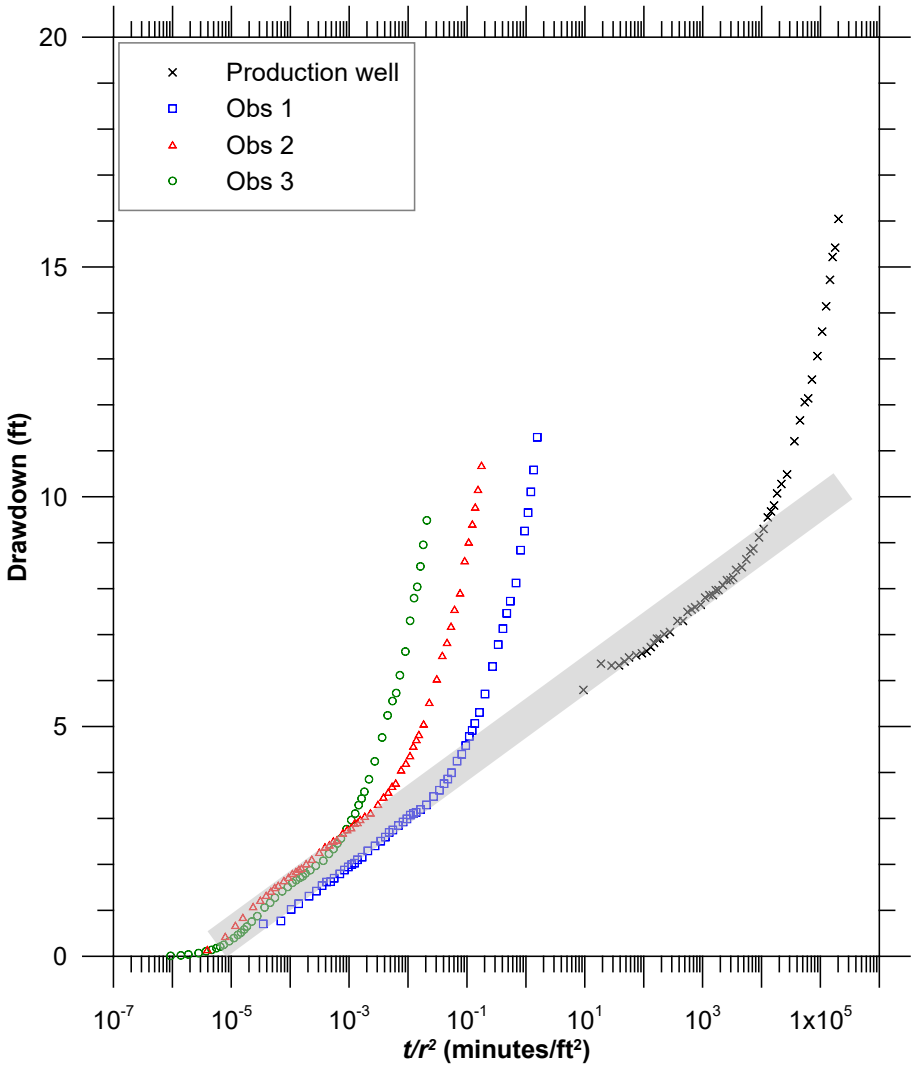

Figure 25. Composite plot with infinite aquifer response

The derivative can also be used to confirm the diagnosis of the early portions of the aquifer response. The "raw" drawdown derivatives for all of the wells are shown in Figure 26. The derivative is calculated using the nearest-neighbor approach.

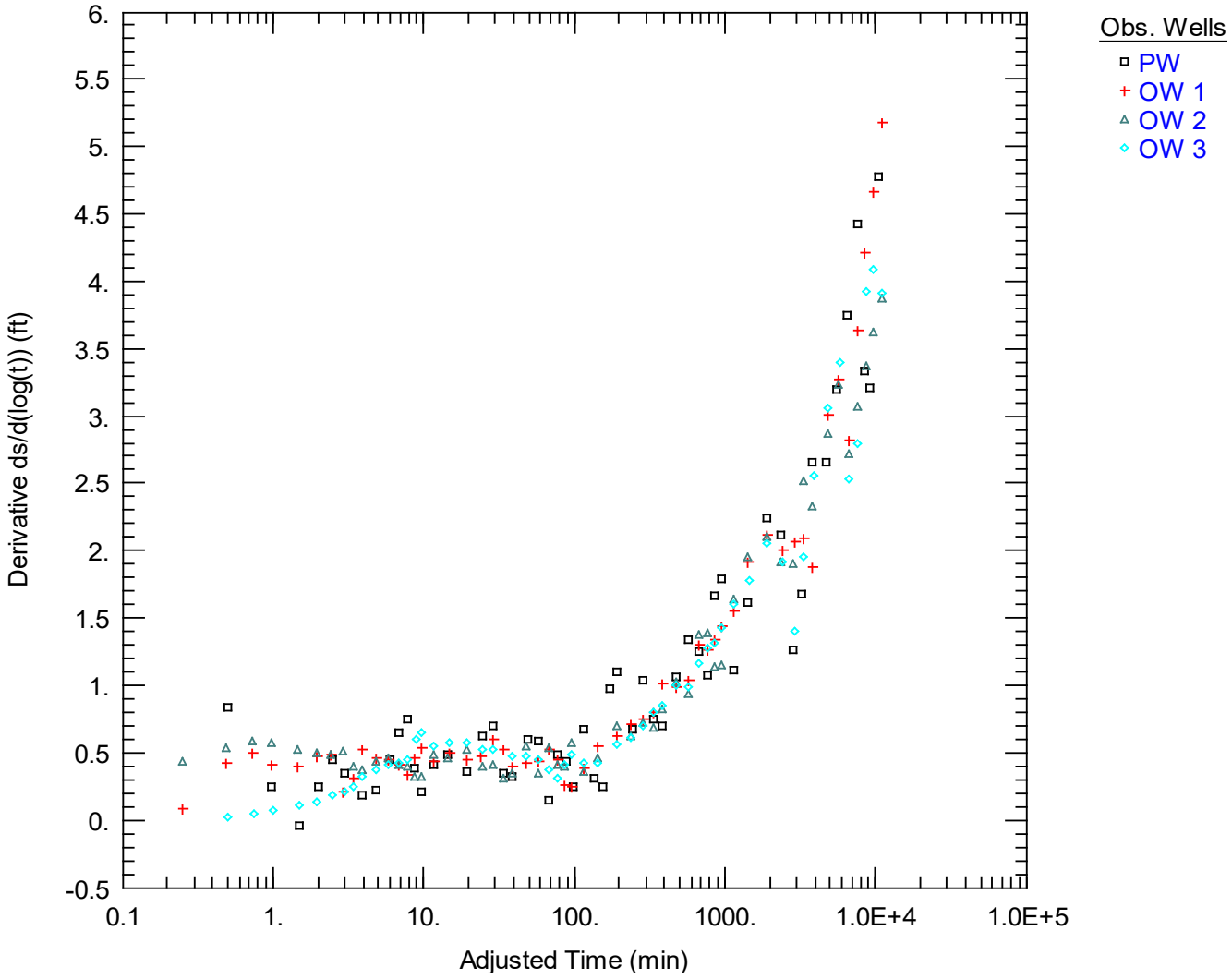

Figure 26. Drawdown derivatives calculated with the nearest neighbour approach

The “raw” drawdown derivatives are not that rough. It is possible to identify gross trends. To improve the visualization, we apply a relatively small amount of smoothing. The “smoothed” drawdown derivatives for all of the wells are shown in Figure 27. We see that the drawdowns reach a plateau between 10 and 100 minutes, followed by a rapid increase. The presence of a plateau suggests that there is a period during which the aquifer responds as if it were unbounded, the period of Infinite Acting Radial Flow (IARF). The increasing rate of change beyond the IARF period is characteristic of a groundwater system with that is enclosed by more than one impermeable boundary.

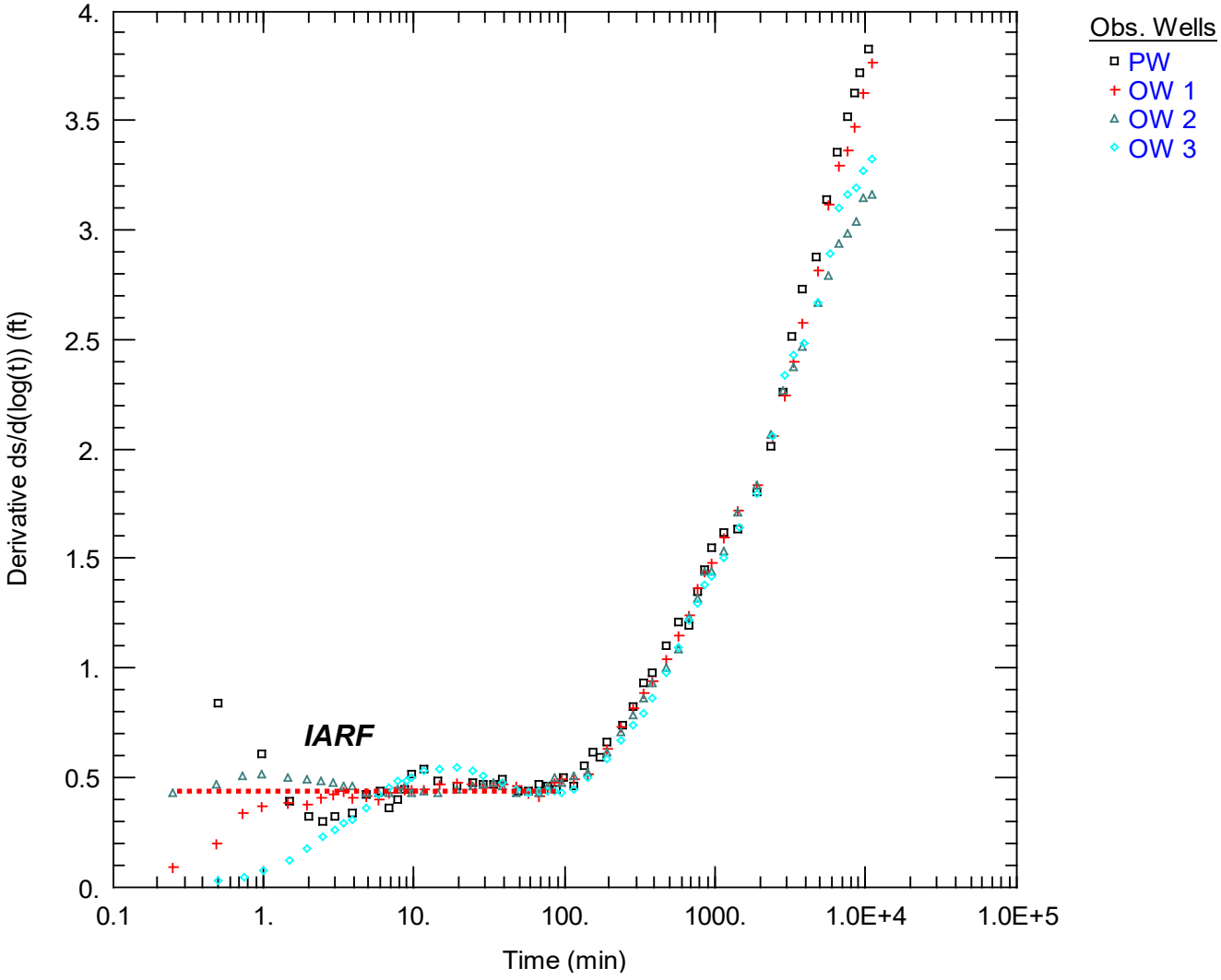

Figure 27. Smoothed drawdown derivatives

Estimation of transmissivity

The Cooper and Jacob straight-line (CJSL) analysis on the composite plot provides a reliable basis for estimating the transmissivity. The slope and intercept of the linear portion of the data are 3.65 ft per $\log_{10}$ cycle of (t/r^2), and $(t/r^2)_0 = 3.0\times10^{-6}$, respectively. When these values are substituted into the Cooper and Jacob formulae, a transmissivity of 21,000 ft^2/d is estimated, along with a storativity of 1.0×10^{-4}.

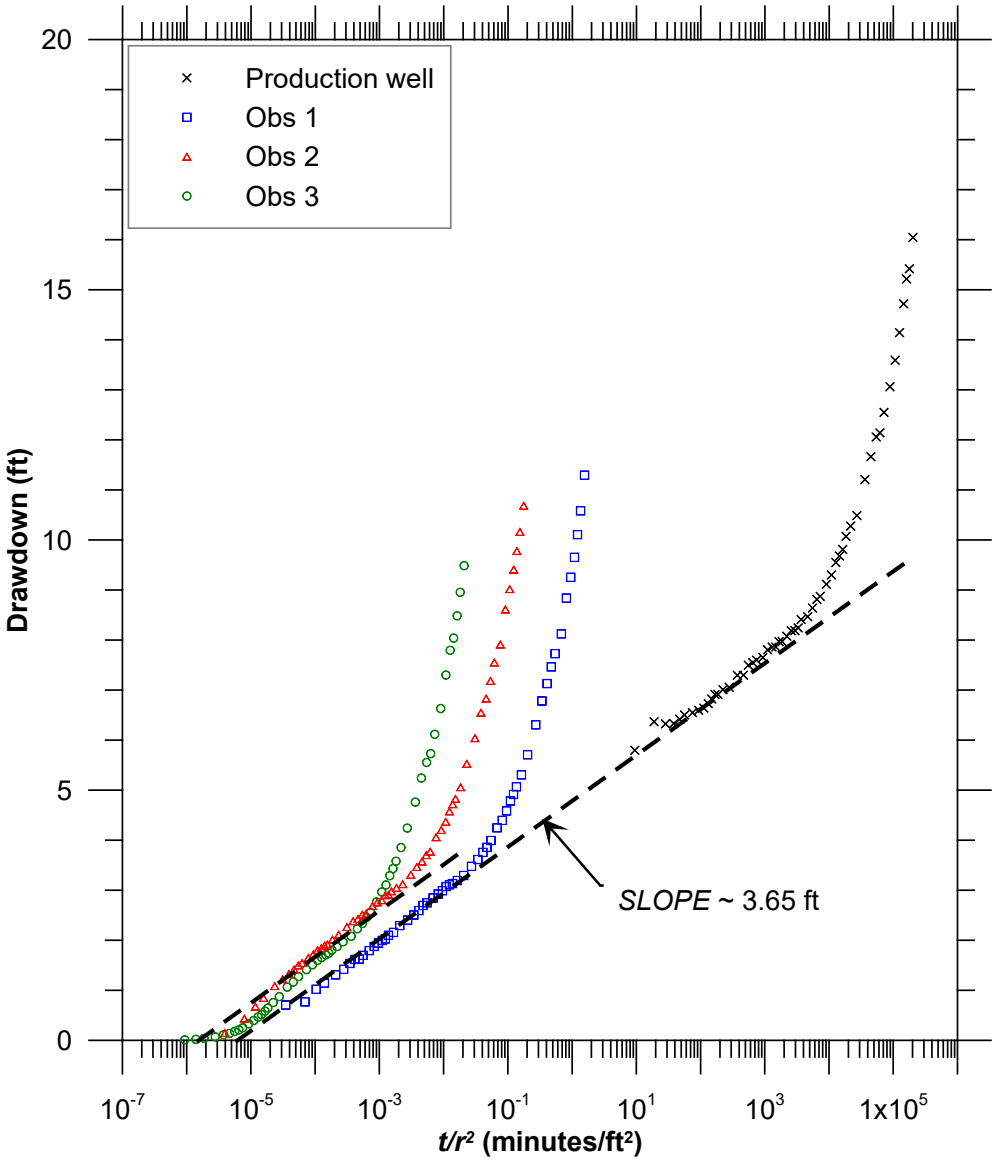

Figure 28. Cooper-Jacob straight-line analysis

As a check on the estimation of the transmissivity and storativity, the estimated parameters are used to calculate the drawdown with the Theis solution. As shown in the log-log composite plot in Figure 29, the match between the theoretical solution and the common portions of the data from each observation well is excellent. The deviations from the Theis curve become very clear when the data are plotted in this format.

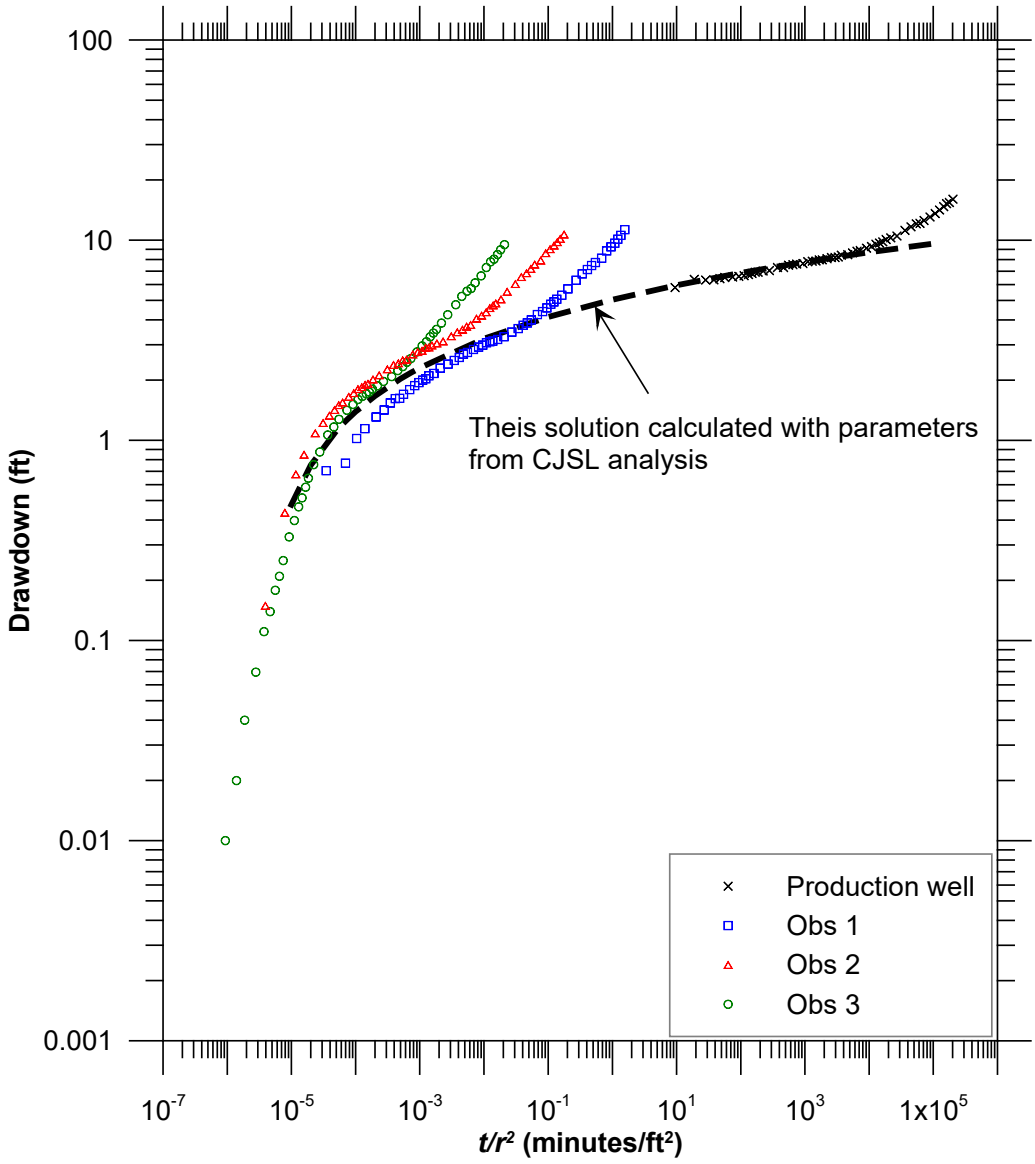

Figure 29. Check on Cooper-Jacob straight-line analysis with Theis solution

Re-analysis of the Estevan test using a channel aquifer model

As a final analysis, we retain the parameter estimates from the Cooper-Jacob analysis in Figure 28, but we invoke the model for a channel aquifer. The only change we make is that we assume the pumping well and observation wells are located in a long channel aquifer with impermeable walls. We don't know how wide the channel is, or where the wells are located with respect to the valley walls. For simplicity, we will assume that the pumping well and the observation wells are located along the axis of the channel (*x*-axis). We will try to estimate the width of the channel through trial-and-error.

For the following trials we retain the transmissivity estimated from the Cooper-Jacob composite analysis.

Run 1: Channel width = 1,000 ft

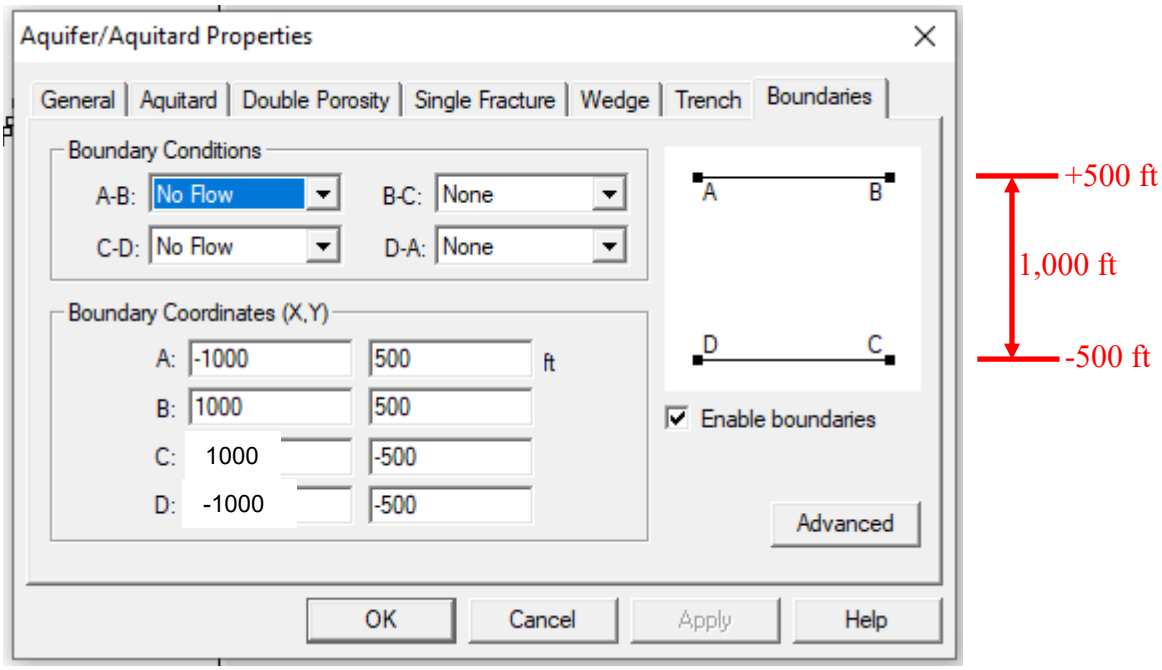

The results of the first guess of the channel width are shown in Figure 29. As shown in the figure, the Theis solution supplemented with image well analysis doesn't match the observations particularly well, but the general trends appear to be correct. We are on to something.

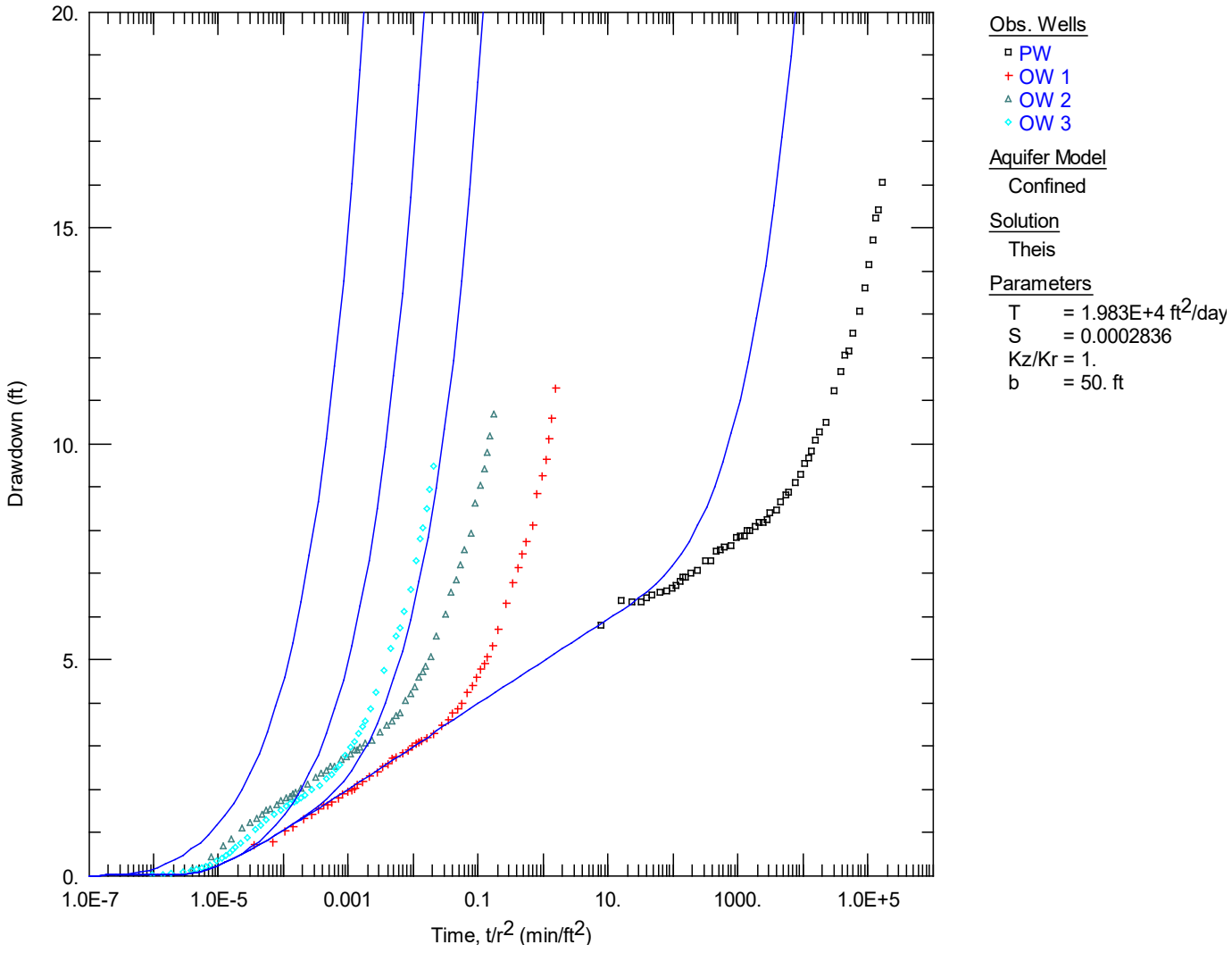

Figure 29. Buried channel analysis for a valley 1,000 ft wide

Run 2: Channel width = 10,000 ft

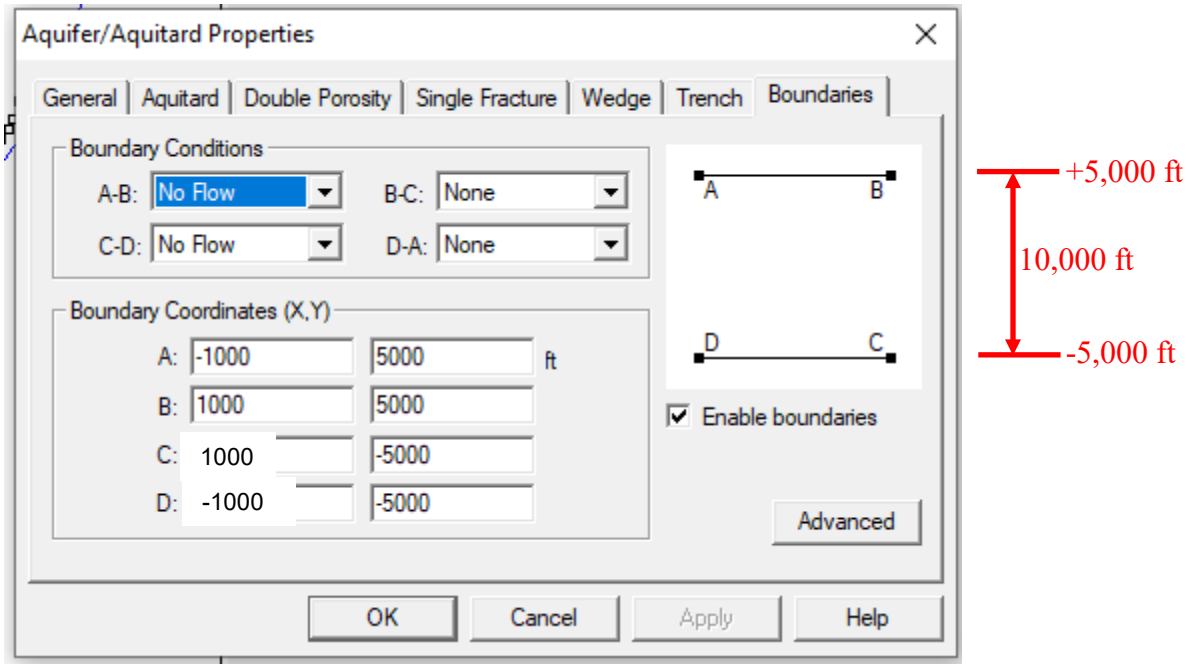

The results of the second guess of the channel width are shown in Figure 30. As shown in the figure, the Theis solution supplemented with image well analysis is much closer to reproducing both the magnitudes and trends of the observed drawdowns. One more trial ought to do it.

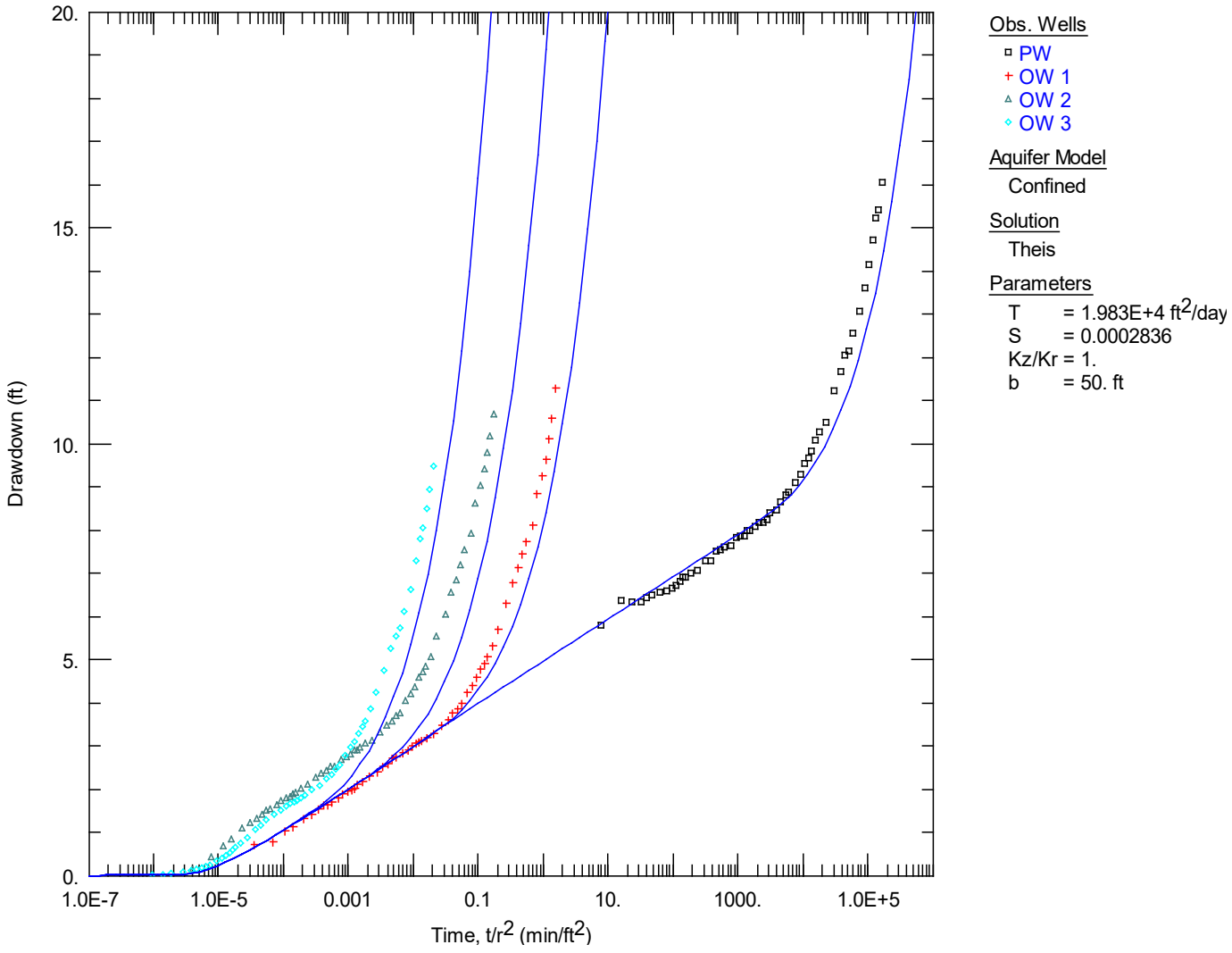

Figure 30. Buried channel analysis for a valley 10,000 ft wide

Run 3: Channel width = 8,000 ft

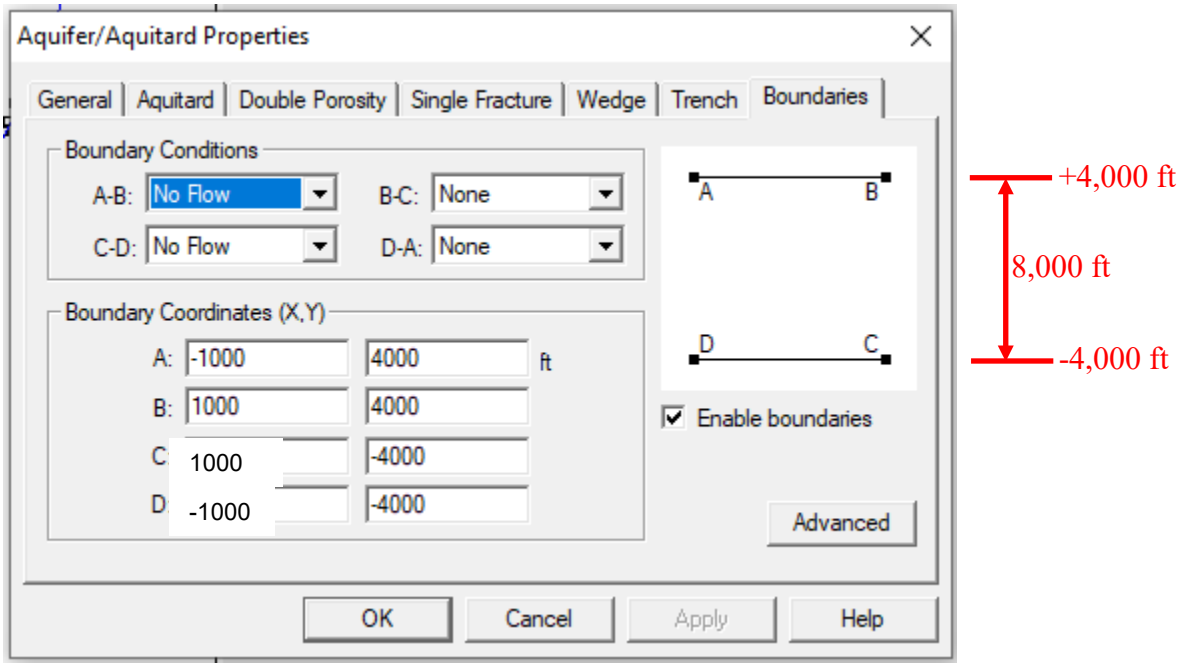

The results of the third guess of the channel width are shown in Figure 31. As shown in the figure, the Theis solution supplemented with image well analysis matches closely the observed drawdowns with the transmissivity estimated from the Cooper-Jacob composite analysis. The corresponding derivative plot is shown in Figure 32. The match to the drawdowns reproduces the key trend in the derivative: a steeply increasing semilog rate of drawdown, with no suggestion of a late-time plateau.

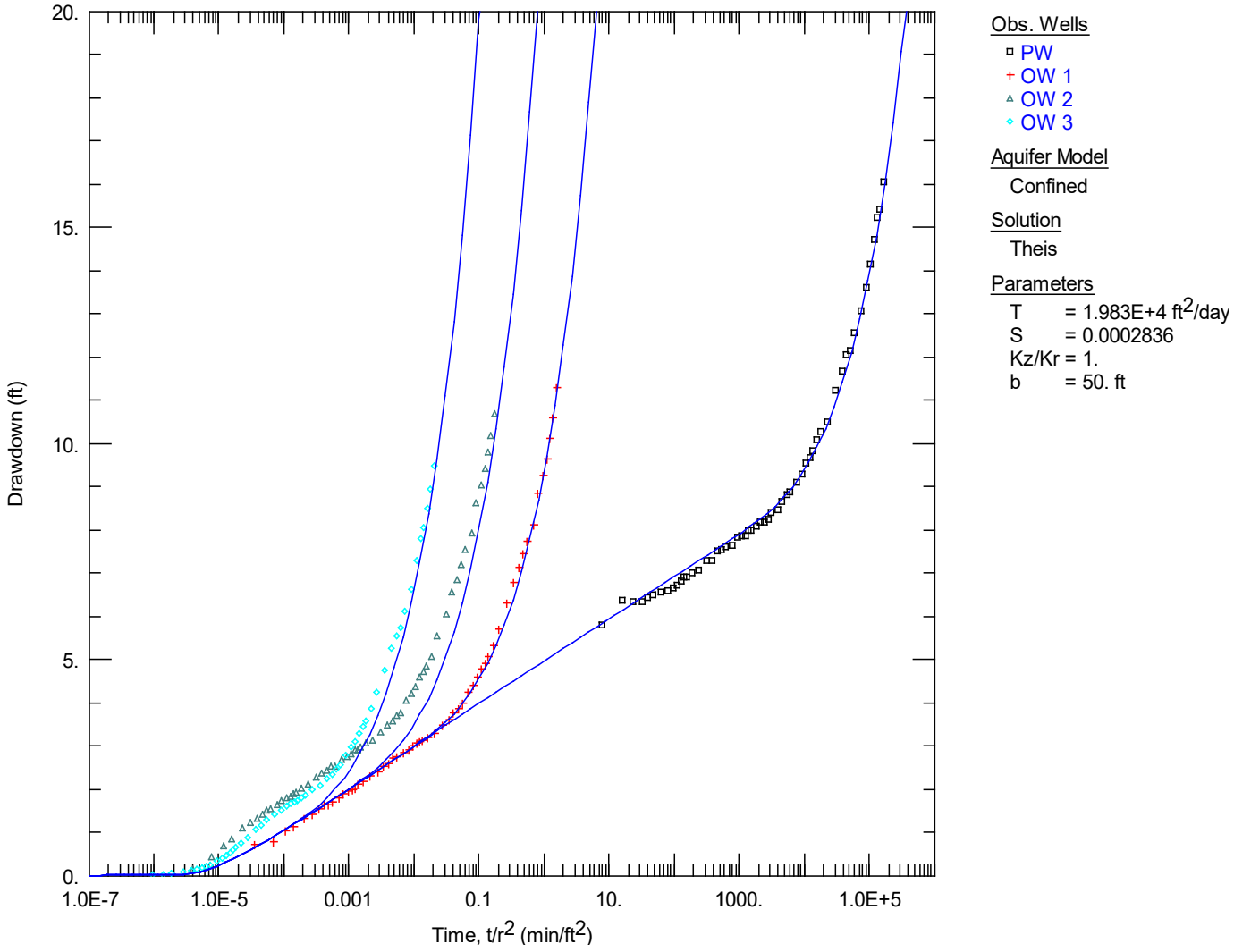

Figure 31. Buried channel analysis for a valley 8,000 ft wide

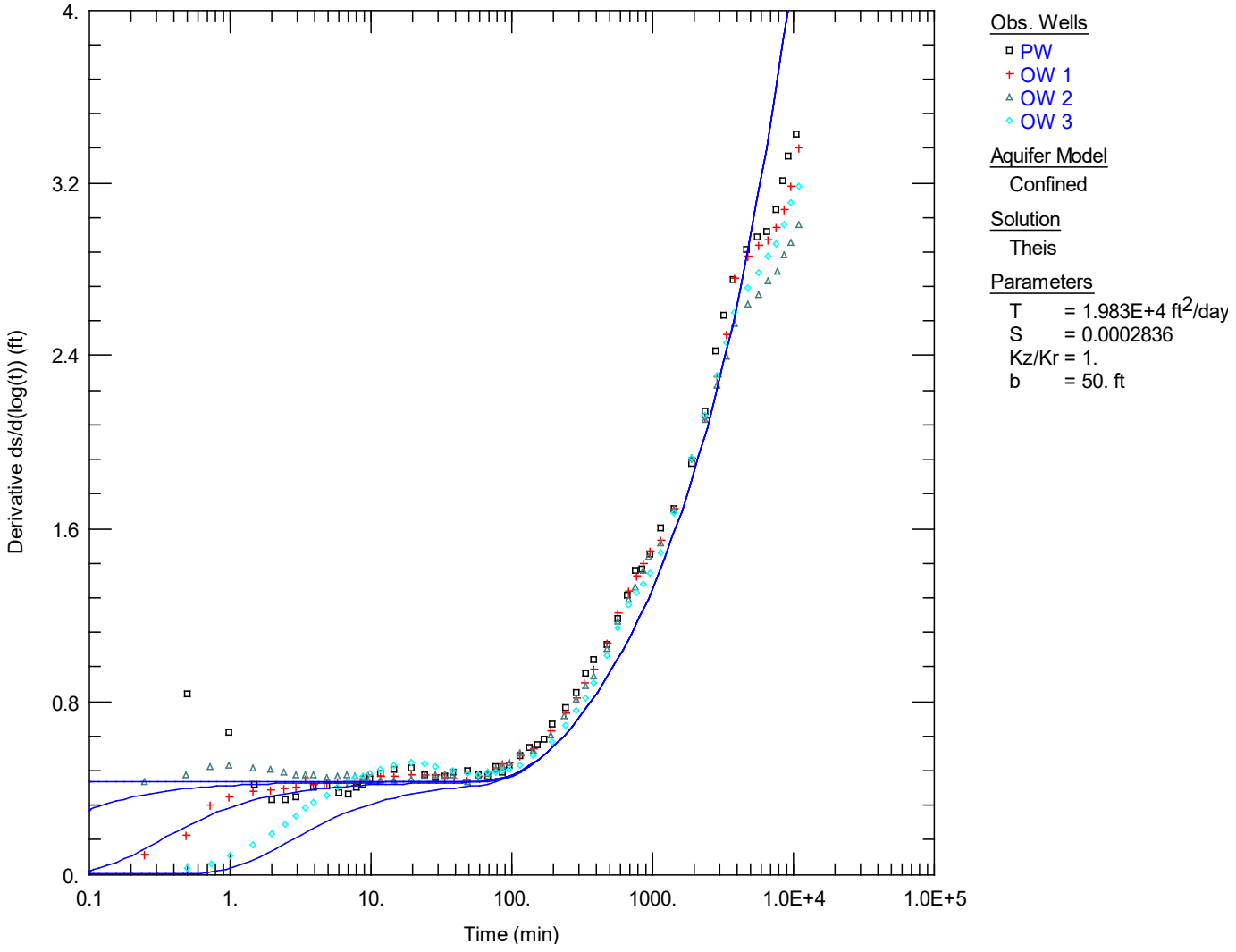

Figure 32. Calculated drawdown derivative for a channel aquifer 8,000 ft wide

6. Key points

1. All aquifers are bounded. In many cases of practical significance, neglecting the boundaries may be highly restrictive.

2. Pumping tests conducted near a linear boundary (for example, a stream or a fault) can be interpreted by superposing Theis solutions in space, using what are referred to as *image wells*.

3. A linear constant-head boundary is simulated with an imaginary well placed an equal distance from the boundary, pumping at a rate equal in magnitude, but opposite in sign, to the actual well.

4. A linear no-flow boundary is simulated with an imaginary well placed an equal distance from the boundary, pumping at a rate equal in magnitude, with the same sign, as the actual well.

5. For a strip aquifer that is bounded on both sides by no-flow boundaries, an infinite number of image wells are required. In practice, the calculations frequently converge to the same result with a relatively small number of image wells.

6. The application of the Derivative Analysis enhances our ability to diagnose the effects of boundaries.

7. The composite plot is an effective method for synthesizing drawdown data and identifying the appropriate portion of the response for the estimation of aquifer properties.

7. References

Betcher, R.N., G. Matile, and G. Keller, 2005: Yes Virginia, there are buried valley aquifers in Manitoba, in *Proceedings of the 58th Canadian Geotechnical and 6th Joint IAH-CNC and CGS Conference*, Saskatoon, Saskatchewan, 6 p.

Cooper, H.H., Jr., and C.E. Jacob, 1946: A generalized graphical method for evaluating formation constants and summarizing well-field history, *Trans. American Geophysical Union*, vol. 27*,* no. 4), pp. 526-534.

Farvolden, R.N., 1963: Bedrock channels of southern Alberta, in *Early Contributions to Groundwater Hydrology of Alberta*, Research Council of Alberta Bulletin 12, pp. 63-75.

Kruseman, G.P., and N.A. de Ridder, 1990: **Analysis and Evaluation of Pumping Test Data**, 2nd ed., International Institute for Land Reclamation and Improvement, Wageningen, The Netherlands.

Maathuis, H., and G. van der Kamp, 2003: Groundwater resource evaluations of the Estevan Valley aquifer in southeastern Saskatchewan: A 40-year historical perspective, in *Proceedings of the 56th Canadian Geotechnical and 3rd Joint IAH-CNC and CGS Conference*, Winnipeg, Manitoba, 4 p.

Motz, L.H., 1991: Aquifer parameters from constant discharge Nonsteady-leaky type curves, *Ground Water*, vol. 29, no. 2, pp. 181-185.

Russell, H.A.J., M.J. Hinton, G. van der Kamp, and D.R. Sharpe, 2004: An overview of the architecture, sedimentology and hydrogeology of buried-valley aquifers in Canada, in *Proceedings of the 57th Canadian Geotechnical and 4th Joint IAH-CNC and CGS Conference*, Québec, Québec, 8 p.

Vandenberg, A., 1977: Type curves for analysis of pump tests in leaky strip aquifers, *Journal of Hydrology*, vol. 33, pp. 15-26.

van der Kamp, G., and H. Maathuis, 2002: The peculiar groundwater hydraulics of buried-channel aquifers, in *Proceedings of the 55th Canadian Geotechnical and 3rd Joint IAH-CNC and CGS Groundwater Specialty Conference*, Niagara Falls, Ontario, pp. 695-698.

van der Kamp, G., and H. Maathuis, 2012: The unusual and large drawdown response of buried-valley aquifers to pumping, *Ground Water*, vol. 50, no. 2, pp. 207-215.

Walton, W.C., 1970: **Groundwater Resource Evaluation**, McGraw-Hill Book Company, New York, New York.

8. Additional readings

1. Ferris, J.G., D.B. Knowles, R.H. Brown, and R.W. Stallman, 1962: excerpt from *Theory of Aquifer Tests*: Theory of Images and Hydrologic Boundary Analysis, United States Geological Survey, Water-Supply Paper 1536-E, pp. 144-166.

2. van der Kamp, G., and H. Maathuis, 2012: The unusual and large drawdown response of buried-valley aquifers to pumping, *Ground Water*, vol. 50, no. 2, pp. 2207-215.

3. Rafini, S., R. Chesnaux, A. Ferroud, 2017: A numerical investigation of pumping-test responses from continuous aquifers, *Hydrogeology Journal*, vol. 25, no. 3, pp. 877-894.